Speed Control of Brushless Dc Engine Using fuzzy Based Show Reference Versatile Control

Article *in* Control and Instrumentation · May 2021

DOI: 10.46610/JOIIS.2021.v06i01.001

2 authors:

Kejela Adane Dulecha
Jimma University
2 PUBLICATIONS **0** CITATIONS
SEE PROFILE

Amruth Ramesh Thelkar
Jimma University
15 PUBLICATIONS **46** CITATIONS
SEE PROFILE

Journal of Instrumentation and Innovation Sciences
e-ISSN: 2456-9860
Volume-6, Issue-1 (January-April, 2021)
www.matjournals.com
https://doi.org/10.46610/JOIIS.2021.v06i01.001

Speed Control of Brushless Dc Engine Using fuzzy Based Show Reference Versatile Control

Kejela Adane Dulecha[1], Amruth Ramesh Thelkar[2 *]
[1]Lecturer, [2]Assistant Professor
[1, 2]Department of Electrical and Computer Engineering, Jimma Institute of Technology, Jimma, Ethiopia

*Corresponding Author: amruth.rt@gmail.com

ABSTRACT
Brushless DC engine drives are broadly utilized in different mechanical frameworks application such as servomotor drives, therapeutic, car and aviation industry. BLDC engines are commutated electronically and offer numerous preferences over brushed DC engines which incorporate expanded productivity, longer life, moo volume and tall torque. Speed control of BLDC engine with radically changing and questionable stack variety with customary PID control framework is incapable to glass up with conjointly incapable to adjust framework stack variety with consistent gain values. So, the most objective of this proposal is to plan a controller to keep the yield speed of the BLDC engine consistent, beneath diverse working conditions such as parameter varieties at evaluated speed, questionable stack unsettling influences and etc. In Fluffy shrewdly controller based demonstrate reference versatile control, the plant yield is shifted with regard to the yield of the reference demonstrate with a few altering components in arrange to get the speed control at working condition. The stage for displaying of BLDC engine and reenactment of the control framework has been done utilizing MATLAB/Simulink Computer program and the result appears that cleverly based demonstrate reference versatile controller is way better in relentless state execution and stack dismissal property than basic MIT run the show and customary PID controller and moved forward the existing framework of the relentless state response.

Keywords-- Brushless DC engines (BLDCM), Fluffy Rationale control (FLC), Demonstrate Reference Versatile Control (MRAC), Lyapunov Soundness Strategy, PID Controller

INTRODUCTION

There are two common place definitions around the brushless DC engine (BLDC engine, BLDCM) have been displayed by distinctive researchers. The as it were trapezoid-wave/square-wave brushless engines may well be called BLDC engines agreeing to analysts, and the sine-wave BLDC engines ought to be called lasting magnet synchronous engines (PMSM) [1-2]. Though, other researchers thought that all the engines over ought to be considered as BLDC engine [3]. BLDCM are powered and run by DC voltage, but current commutation is achieved by electric commutation system which is solid state current commutation. Therefore, the BLDC motor has been used in many applications such as electric automotive, robotics, HVAC, electronics, computer, semiconductor, CD-ROMS, medical industries, feed drives for CNC machines, extruder drives and so on. Due to long operating life, High dynamic response, High efficiency, Better speed vs torque characteristics, higher speed range and higher torque–weight ratio and in such applications BLDC motor exposed too many kinds of load disturbances. Conventional controlling methods couldn't achieve the required speed and tracking response with stable good accuracy in the condition of sudden disturbance and parameter variations [9-10]. This issue can be illuminated by utilizing progressed control methods such as versatile control, variable structure control, fluffy control and neural organize control [4].

https://doi.org/10.46610/JOIIS.2021.v06i01.001

They offered BLDC motor tracking control using self-tuning fuzzy PID control and model reference adaptive control and the paper relates the performance of two different control techniques applied to high performance brushless DC motor and they used self-tuning fuzzy PID controller and adaptive MRAC controller with PID compensator to achieve for different speed/time tracks regardless of load disturbance and parameter variation and their control system have better performance but they ignored load disturbance and input variation and they have used additional PID compensator[11-12] [14]. They proposed a controller and designed to regulate the speed of BLDC motor using a conventional PID control technique and also a control technique with model reference adaptive control is used and still the proposed system have considerable percentage overshoot and high rise and settling time when compared with a conventional controller [10]. They proposed Demonstrate Reference Versatile Control for BLDC engines and planned with a PID controller tuned by GA-ANFIS. GA-Trained ANFIS system for tuning the PID controller has been proposed [13-23]. This is often utilized at the side the MRAC to provide improved execution within the control of BLDC engine and the performance is validated against convention PID and self-tuning PID controllers. The result demonstrates a superior performance of the proposed approach but still they used an extra compensator to tune a PID controller and didn't consider uncertain load disturbance [13].

Whereas, the basic problems in using a conventional PID controller in a position or speed control are the effects of nonlinearity in a DC motor as well as controllability effect [24]. Hereditary Calculation is proposed as a worldwide optimizer to discover optimized PID picks up for position control of BLDC motor [5]. It encompasses an impediment of high-power utilization. Utilizing fluffy rationale as a plan strategy, this can be connected in creating nonlinear framework for implanted control. A single set of Fuzzy rules were utilized for controlling values within the controller so it fizzled to adjust with alter in parameters [6]. The controller is designed to regulate and robust the speed of BLDC motor using a conventional PID control technique and a control technique with model reference adaptive control and also a fuzzy control technique for error reduction by minimizing steady state error as well as percentage over shoot is used for the design system. Therefore, in this paper three advanced control strategies are going to be adopted and compared. The primary control method is routine PID controller which appears a great execution compared to the other ordinary controller the moment strategy is based on MRAC framework and having MRAC system on the plant shows a reasonable performance but it has comparative rise time and steady state error [7]. The third technique is combining MRAC with fuzzy control theory which minimizes both the overshoots and steady state error of the control system and has ability to reject load disturbance with adapting mechanism and sustain motors long operating life as advantage [8]. Hence, the fundamental errand is to design such a control, which can guarantee the negligible blunder between the reference show and the plant yields in spite of the instabilities or varieties within the plant parameters and working conditions. The primary approach is to plan a show reference versatile controller utilizing Fluffy based on Lyapunov steadiness hypothesis strategy. This hypothesis guarantees that the system at balance point is asymptotically steady and is favored for a moment arrange framework because it surrender way better execution than MIT Run the show.

MATHEMATICAL MODEL OF BLDC MOTOR

Transfer Function

Exchange work is one of the foremost crucial thought within the control hypothesis and the exchange function-based displaying are broadly utilized in programmed control areas of plan and control of a plant framework. A few control plan and investigation strategies, such as the root-locus strategy and the frequency-response strategy are moreover created based on the exchange work. Assume that the three-phase BLDC motor is controlled by the full-bridge driving within the two-phase conduction mode and when wending of stage, A and B are conducting their exist [16-19] shown in fig.1.

https://doi.org/10.46610/JOIIS.2021.v06i01.001

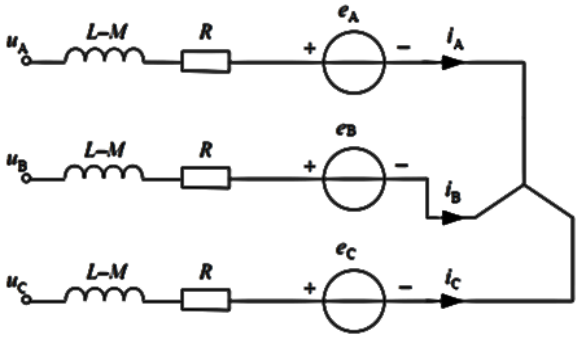

Figure 1: *Equivalent circuit of the BLDC motor*. [15]

The Phase current of the equivalent circuit of the BLDC motor is

$$u_A = Ri_A + (L - M)\frac{di_A}{dt} + + e_A \qquad (1)$$

Then, the matrix form of phase voltage equation of BLDC motor can be expressed as:

$$\begin{matrix} u_A \\ u_B \\ u_C \end{matrix} = \begin{bmatrix} R & 0 & 0 \\ 0 & R & 0 \\ 0 & 0 & R \end{bmatrix}\begin{bmatrix} i_A \\ i_B \\ i_C \end{bmatrix} + \begin{bmatrix} L-M & 0 & 0 \\ 0 & L-M & 0 \\ 0 & 0 & L-M \end{bmatrix}\frac{d}{dt}\begin{bmatrix} i_A \\ i_B \\ i_C \end{bmatrix} + \begin{bmatrix} e_A \\ i_B \\ i_C \end{bmatrix} \qquad (2)$$

The line voltage equation can be obtained through subtraction calculation of the phase voltage equation as:

$$\begin{matrix} u_{AB} \\ u_{BC} \\ u_{CA} \end{matrix} = \begin{bmatrix} R & -R & 0 \\ 0 & R & -R \\ -R & 0 & R \end{bmatrix}\begin{bmatrix} i_A \\ i_B \\ i_C \end{bmatrix} + \begin{bmatrix} L-M & M-L & 0 \\ 0 & L-M & M-L \\ M-L & 0 & L-M \end{bmatrix}\frac{d}{dt}\begin{bmatrix} i_A \\ i_B \\ i_C \end{bmatrix} + \begin{bmatrix} e_A - e_B \\ i_B - e_C \\ i_C - e_A \end{bmatrix} \qquad (3)$$

In order to build a complete mathematical model of the electromechanical system, the motion equation has to be included as:

$$T_e - T_L = J\frac{d\Omega}{dt} + B_V\Omega \qquad (4)$$

Where,

T_L --------- load torque;

J ---------- Rotor moment of inertia;

B_V -------- Viscous friction coefficient $\left\{ \begin{matrix} i_A = -i_B = i \\ \frac{di_A}{dt} = -\frac{di_B}{dt} = \frac{di}{dt} \end{matrix} \right\}$ (5)

Thus, the line-voltage U_{AB} in Equation (3) can be rewritten as:

$$U_{AB} = 2Ri + 2(L - M)\frac{di}{dt} + (e_A - e_B) \qquad (6)$$

Take the transient process out of consideration (i.e. ignore the trapezoid bevel edge), then the steady e_A and e_B are equal in amplitude and opposite in direction when phases A *and* Bturned on. So, Equation (6) can be expressed as:

$$U_{AB} = U_d = 2Ri + 2(L - M)\frac{di}{dt} + 2e_A = r_a i + L_a\frac{di}{dt} + K_e\Omega \qquad (7)$$

Where,

U_d------ DC bus voltage;

r_a -------Line resistance of winding,$r_a = 2R$

L_a -----Equivalent line inductance of winding,$L_a = 2(L - M)$;

K_e -----Coefficient of line back-EMF,

$K_e = 2p\psi_m = 4pNSB_m$.

https://doi.org/10.46610/JOIIS.2021.v06i01.001

Equation (7) is exactly the armature voltage loop equation when two phase windings are excited. Note that the equivalent circuit shown in Fig. 2 could be adopted in three-phase half bridge driving and three-phase full-bridge driving modes of the BLDC motor with specific $k_e$and K_T too.

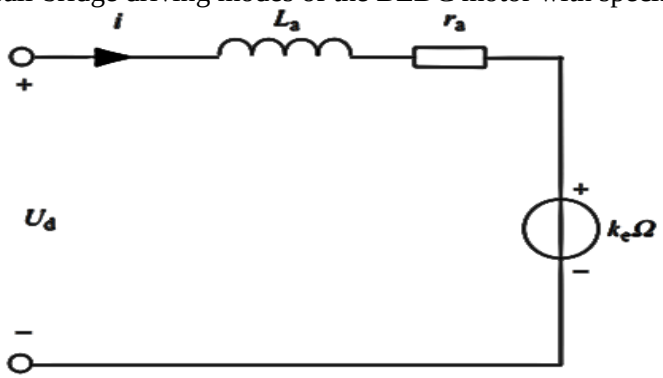

Figure 2: *Equivalent circuit of the BLDC motor with two phase windings excited.* [15]

In Equation (7), if the current can be expressed by angular velocity, then we can get the transfer function of motor by obtaining the relationship between bus voltage and angular velocity.

$$K_T i - T_L = J\frac{d\Omega}{dt} + B_V\Omega \qquad (8)$$

First, when the BLDC motor runs with no load, the current is given as:

$$i = \frac{J}{K_T}\frac{d\Omega}{dt} + \frac{B_V}{K_T}\Omega \qquad (9)$$

Substituting Equation (9) into Equation (7), we get$U_d = r_a\left(\frac{J}{K_T}\frac{d\Omega}{dt} + \frac{B_V}{K_T}\Omega\right) + L_a\frac{d}{dt}\left(\frac{J}{K_T}\frac{d\Omega}{dt} + \frac{B_V}{K_T}\Omega\right) + K_e\Omega$ (10)

Also, it can be rearranged as:

$$U_d = \frac{L_aJ}{K_T}\frac{d^2\Omega}{dt^2} + \frac{r_aJ + L_aB_V}{K_T}\frac{d\Omega}{dt} + \frac{r_aB_V + k_eK_T}{K_T}\Omega \qquad (11)$$

By Laplace transformation of Equation (11), the transfer function of a BLDC motor can be expressed as:

$$G_u(s) = \frac{\Omega(s)}{U_d(s)} = \frac{K_T}{L_aJS^2 + (r_aJ + L_aB_V)s + (r_aB_V + k_eK_T)} \qquad (12)$$

In this way, the structure of a BLDC engine control framework with no stack can be built as appeared in Fig. 3.

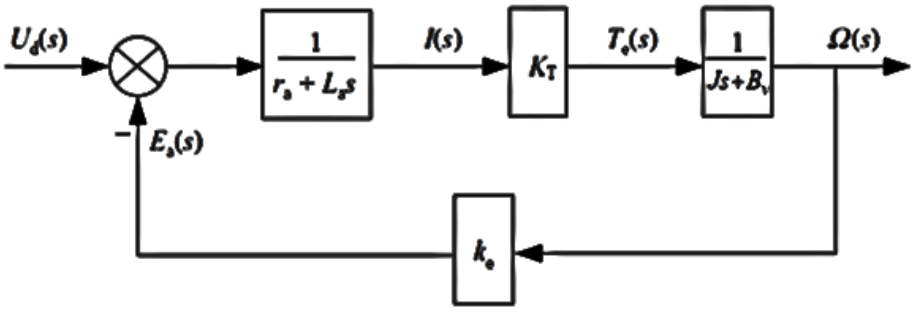

Figure 3: *Structure of BLDC motor with no load control system.*

Equation (12) implies that the BLDC motor can be considered as a second-order system, so it can be rearranged as:

$$G_u(s) = \frac{K_T}{r_aB_V + k_eK_T}\frac{\omega_n^2}{(s^2 + 2\xi\omega_n s + \omega_n^2)} \qquad (13)$$

Where;

https://doi.org/10.46610/JOIIS.2021.v06i01.001

$\omega_n = \sqrt{\frac{r_aB_V+k_eK_T}{L_aJ}}$ ----- Natural frequency of the second-order system;
$\xi = \frac{1}{2}\frac{r_aJ+L_aB_V}{\sqrt{L_aJ}\sqrt{(r_aB_V+K_eK_T)}}$ ------ damping ratio of the second-order system.

It can be seen from Equation (13) that the two roots of the characteristic equation for the BLDC motor's second-order system are $s_{1,2} = -\xi\omega_n \pm \omega_n\sqrt{\xi^2-1}$so the system response time is determined by ω_n and ξ. For unit step input, the convergence speed of the response curve depends on ω_n.A larger ω_n generally leads to a faster convergence speed. Meanwhile, the parameter ξ will determine the character of eigenvalues and the shape of the response curve. Let the mechanical time constant be$t_m = \frac{r_aJ+L_aB_V}{r_aB_V+k_eK_T}$ and the electromagnetic time constant be
$t_e = \frac{L_aJ}{r_aJ+L_aB_V}$ Then Equation (14) can be rewritten as:

$$G_u(s) = \frac{K_T}{r_aB_V + k_eK_T}\frac{1}{(s^2t_mt_e + st_m + 1)} \qquad (14)$$

Generally speaking, the mechanical time constant is much larger than the electromagnetic time constant, i.e.$t_m \gg t_e$, so the transfer function expressed in Equation (14) further can be simplified as

$$G_u(s) = \frac{K_T}{r_aB_V + k_eK_T}\frac{1}{(s^2t_mt_e + st_m + 1)}$$
$$= \frac{K_T}{r_aB_V + k_eK_T}\frac{1}{(st_m+1)(st_e+1)} \qquad (15)$$

It is seen from Equation (15) that the transfer function of BLDC motor can be expressed by two inertia elements in series [20]. Fig. 4 has shown the interconnection between armature current and angular speed. If the effect of electromagnetic time constant is ignored, i.e. the armature inductance is negligible, and then$L_m$can be deemed to be zero, so Equation (14) can be simplified into a first order model as:

$$G_u(s) = \frac{K_T}{r_aB_V + k_eK_T}\frac{1}{(st_m+1)} \qquad (16)$$

The corresponding system structure diagram is shown in Fig. 4. Further, the step response of Equation (16) is given by:-

$$\Omega(t) = \frac{K_TU_d}{r_aB_V + k_eK_T}\left(1 - e^{-t/t_m}\right) \qquad (17)$$

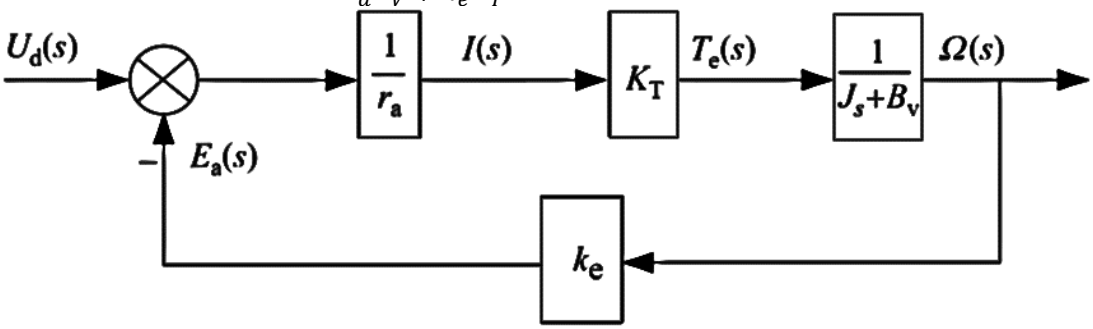

Figure 4: *System structure diagram of BLDC motor with the armature inductance neglected.*

For a speed-control system, it is desirable that the delay time of speed response be short enough. If the mechanical time constant is big, a rational closed control system should be designed to increase the response speed therefore, the stability and the system response speed should be considered together in system design. The response speed should be increased under the condition of stability.

In the following, the transfer function and speed step response of a BLDC motor when the load torque is not zero will be discussed. In this condition, the load torque can be regarded as an input load variation of the system. For such a system, the

https://doi.org/10.46610/JOIIS.2021.v06i01.001

superposition principle holds. Thus, the output of the system equals the sum of out puts when $U_d(s)$ and $T_L(s)$are applied to the system, respectively. In Fig. 5, when$U_d(s) = 0$ holds, hence,

$$\Omega(s) = {}^{1}/_{Js + B_V}\left[-k_e \frac{1}{r_a + L_a s} K_T \Omega(s) - T_L(s)\right] \quad (18)$$

$$\frac{T_L(s)}{} = -\Omega(s)\left[\frac{(r_a + L_a s)(Js + B_{V)} + k_e K_K}{(r_a + L_a s)}\right] \quad (19)$$

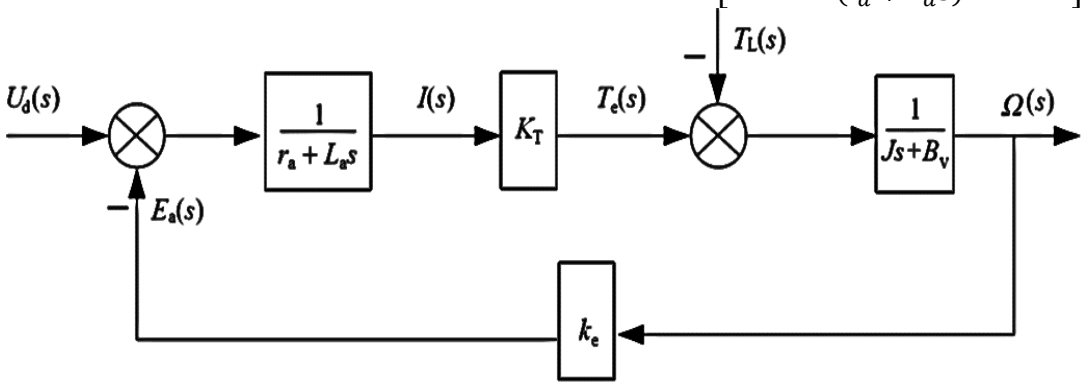

Figure 5: *Structure diagram of BLDC motor with load torque.*

Then, the transfer function between load torque and speed is:

$$G_L(s) = \frac{\Omega(S)}{T_L(s)} = -\frac{r_a + L_a s}{L_a J s^2 + \left(r_{aJ} + L_{aB_V}\right)s + (r_a B_V + k_e K_T)} \quad (20)$$

Therefore, the speed response of a BLDC motor affected together by voltage and load torque is given by:

$$\Omega(s) = G_d(s)U_d(s) + G_L(s)T_L(s)$$

Then;

$$\Omega(s) = \frac{K_T U_d(s)}{L_a J S^2 + (r_a J + L_a B_V)s + (r_a B_V + k_e K_T)} - \frac{(r_a + L_a s)T_L(s)}{L_a J s^2 + \left(r_{aJ} + L_{aB_V}\right)s + (r_a B_V + k_e K_T)} \quad (21)$$

CONTROLLER DESIGN
PID Controller

PID has wide industrial applications as it need only less parameter to be tuned. It abolishes the steady state error by integral action and anticipates the change in output by derivative action. For tuning of parameters in PID controller a lot of techniques are available. Zeigler Nicholas Tuning method is the most popular method for tuning of PID controller. It depends mainly on step response of the system. The standard PID controller calculates the deviation e(t) between the reference value and the actual value. Then, the plant is controlled by the variable u(t) with a linear combination of proportional-integral-derivative terms. The corresponding PID control law in continuous form can be expressed as:

$$\mathrm{u(t)} = K_P\left(e(t) + \frac{1}{T_I}\int_0^t e(t)\,dt + T_D\frac{de(t)}{d(t)}\right) \quad (22)$$

The typical structure of PID control of BLDC is shown in Fig. 6.

https://doi.org/10.46610/JOIIS.2021.v06i01.001

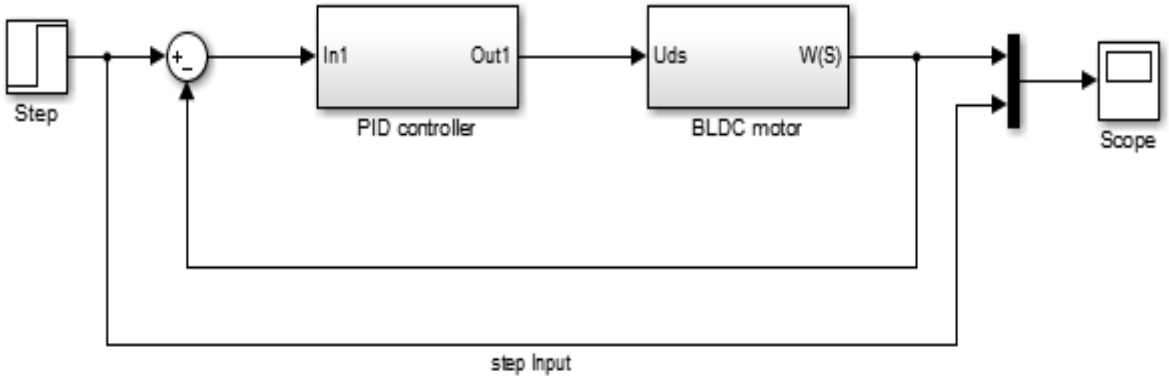

Figure 6: *Diagram of a PID control system of BLDC motor.*

The differential term can successfully decrease the overshoot and greatest energetic deviation, but it'll make the controlled plant effectively influenced by high-frequency unsettling influences. And the Simulink square graph of the PID control framework is given underneath in Fig. 7.

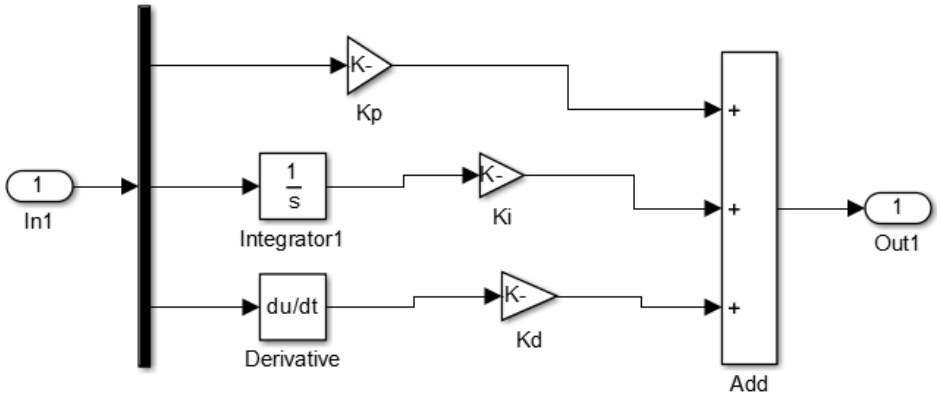

Figure 7: *Internal Simulink block diagram of PID controller Structure.*

Zeigler Nicholas Method

From Fig. 7 of the PID control structure diagram the Ziegler Nicholas method calculation is derived below and our goal is to choose K_p,K_I, and K_d values appropriately by using oscillation.

Ziegler Nichols is an iterative, online method to choose each value and there is no need of modeling required therefore, from equation (22) U(t) is derived:

$$u(t) = k_p e(t) + \frac{k_p}{T_i}\int_0^t e(t)d(t) + k_p T_d \frac{de(t)}{d(t)} \qquad (23)$$

From equation (23), K_I and K_d values are from those values Ti and Td:

$$K_I = \frac{k_p}{T_i}\int_0^t e(t)d(t) \qquad (24)$$

$$K_d = k_p T_d \frac{de(t)}{d(t)} \qquad (25)$$

To determine the Ziegler Nichols parameters for a PID controller, by oscillation method and adjusting the parameter until we get a certain critical system and adjusting the parameters within the simulation and based on the Ziegler Nichols Table 1 below, we find out the parameters as given below.

https://doi.org/10.46610/JOIIS.2021.v06i01.001

Table 1: *Ziegler Nichols parameters.*

Controller	Kc	τ_i	τ_d
P	0.5Kcu	-	-
PI	0.455Kcu	0.83Pu	-
PID	0.6Kcu	0.5Pu	0.125Pu

From the table and oscillation method we determined the period or the oscillation period of the PID tuner w=0.5403, hence the ultimate gain or frequency is given as:

$P_U = \frac{2\pi}{w} = 2 * \frac{3.14}{0.5403} = 11.623$ And Kcu=1.491 obtained from oscillation method.

$\tau_i = 0.5Pu = 0.5 * 11.623 = 5.8115$

$\tau_d = 0.125 * 11.623 = 1.453$

From equation (24) and (25).

PID controller gain parameter with small and small value estimation is given by:

k_p=5.7748, K_I=1605.29 and K_d=0.00468 which is a tray and error method mostly.

Model Reference Adaptive Controller

Versatile Control handle is the one that persistently and naturally measures the energetic behavior of plant, compares it with wanted yield and employments the distinction to differ flexible framework parameters or to produce the inciting flag in such a way as to get ideal execution [21-22]. A versatile control framework has two circles. One is the standard feedback with get ready and controller and the other circle comprises of the modification circle. The parameter change circle is routinely slower than the standard input circle. It can adapt to any alter within the speed which happens due to variety in stack or due to outside unsettling influences and the show reference versatile controller primary framework piece chart is given underneath in Fig. 8.

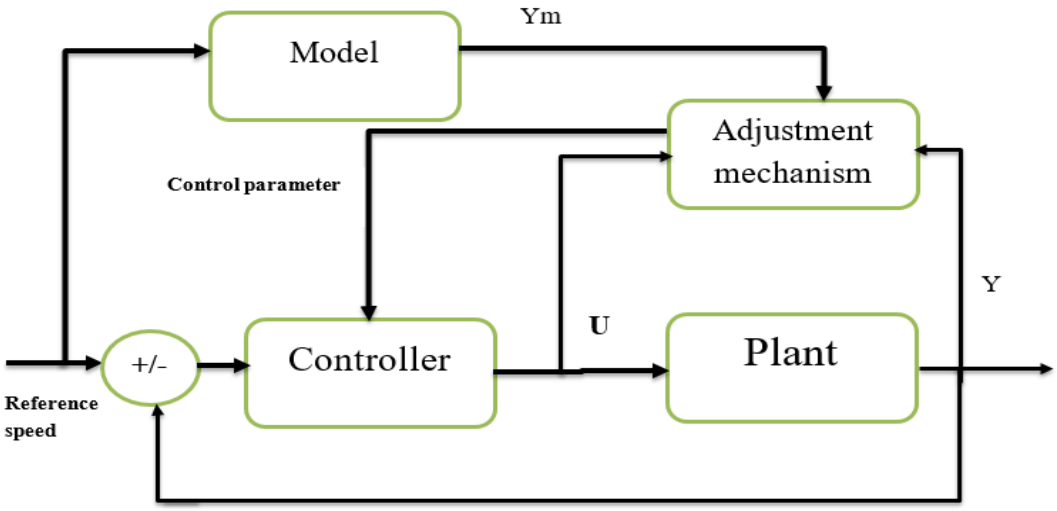

Figure 8: *Block diagram of a model reference adaptive system (MRAC).*

In demonstrate reference versatile controller, controller is planned to drive the framework or plant to act like reference demonstrate. Show yield is compared to the real yield, and the contrast is utilized to alter the input controller parameters MRACS has two circles i.e. internal circle a conventional control circle comprising of plant and controller, an external circle or adjustment circle that alter the control.

MRAC Based MIT Rule

This run the appear is made in Massachusetts Built up of development and is utilized to apply the MRAC approach to any down to soil system. In this run the show the fetched work or misfortune work is characterized as angle error.

https://doi.org/10.46610/JOIIS.2021.v06i01.001

$$J(\theta) = {}^{1}/_{2}\, e^2 \qquad (26)$$

The fractional subsidiary term ∂e/ ∂θ, is called the affectability subordinate of the framework. This appears how the mistake is subordinate on the flexible parameter θ. There are numerous options to select the misfortune work J, like it can be taken as mode of blunder too. Similarly, dθ/dt, can moreover have distinctive relations for distinctive applications. Required general MIT gradient equations:

Process: $\boldsymbol{G(s)} = \frac{\boldsymbol{y}}{\boldsymbol{u}}$ (27)

Model: $\boldsymbol{G_m(s)} = \frac{\boldsymbol{y_m}}{\boldsymbol{r}}$ (28)

Control law: $\boldsymbol{u(t)} = \boldsymbol{f(u_c, y)}$ (29)

Get Close loop from (27) and (29): $\frac{\boldsymbol{y}}{\boldsymbol{r}}$ (30)

Error: $e = y - y_m$ (31)

$$\frac{\partial e}{\partial \Theta} = \frac{\partial y}{\partial \Theta} \qquad (32)$$

MIT rule: $\frac{d_\theta}{dt} = -\gamma e \frac{\partial e}{\partial \Theta} = -\gamma e \frac{\partial y}{\partial \Theta}$ (33)

The BLDC motor process is a second order element with the following transfer function:
From equation (13):

$$G_u(s) = \frac{K_T}{r_a B_V + k_e K_T} \frac{\omega_n^2}{(s^2 + 2\xi\omega_n s + \omega_n^2)}$$
$$= \frac{\alpha_1}{s^2 + \alpha_2 s + \alpha_3} \qquad (34)$$

For the reference model, a second order transfer function is selected as:

$$G_m(s) = \frac{y_m(s)}{r(s)} = \frac{\omega_n^2}{s^2 + 2\xi\omega_n s + \omega_n^2} \qquad (35)$$

The control law is chosen as:

$$u(t) = k_1 r(t) - k_2 y(t) - k_3 \dot{y(t)} \qquad (36)$$

The MIT rule is applied, where p is the differential operator which is P=S therefore y (t) becomes:

$$y(s) = G_u(s)u(s) = \frac{\alpha_1}{s^2 + \alpha_2 s + \alpha_3}(k_1 R(s) - k_2 y(s) - k_3 s\dot{y(s)})$$
$$y(s) = \frac{\alpha_1 K_1 R(s)}{s^2 + (\alpha_2 + \alpha_1 k_3)s + \alpha_3 + \alpha_1 k_2}$$
$$y(t) = \frac{\alpha_1 K_1 r(t)}{p^2 + (\alpha_2 + \alpha_1 k_3)p + \alpha_3 + \alpha_1 k_2} \qquad (37)$$

As a consequence, the error is:

$$e = y - y_m$$
$$e(t) = \left(\frac{\alpha_1 K_1 r(t)}{p^2 + (\alpha_2 + \alpha_1 k_3)p + \alpha_3 + \alpha_1 k_2} - \frac{\omega_n^2}{s^2 + 2\xi\omega_n s + \omega_n^2}\right) r(t) \qquad (38)$$

The sensitivity derivatives are obtained by taking the partial derivatives of the error and considering the controller parameters:
Therefore:

$$\frac{\partial e}{\partial k_1} = \frac{\alpha_1 r(t)}{p^2 + (\alpha_2 + \alpha_1 k_3)p + \alpha_3 + \alpha_1 k_2} \equiv y_m \qquad (39)$$
$$\frac{\partial e}{\partial k_2} = \frac{-{\alpha_1}^2 k_1 r(t)}{(p^2 + (\alpha_2 + \alpha_1 k_3)p + \alpha_3 + \alpha_1 k_2)^2}$$
$$= -\frac{\alpha_1 y(t)}{p^2 + (\alpha_2 + \alpha_1 k_3)p + \alpha_3 + \alpha_1 k_2} \qquad (40)$$

https://doi.org/10.46610/JOIIS.2021.v06i01.001

$$\frac{\partial e}{\partial k_3} = \frac{-\alpha_1{}^2 p k_1 r(t)}{(p^2 + (\alpha_2 + \alpha_1 k_3)p + \alpha_3 + \alpha_1 k_2)^2}$$
$$= -\frac{\alpha_1 \dot{y}(t)}{p^2 + (\alpha_2 + \alpha_1 k_3)p + \alpha_3 + \alpha_1 k_2)^2} \quad (41)$$

Due to the fact that the process parameters are unidentified, none of the above three equations can be used. The below approximation is required in order to overcome such an impediment:

$$p^2 + (\alpha_2 + \alpha_1 k_3)p + \alpha_3 + \alpha_1 k_2$$
$$p^2 + 2\xi\omega_n p + \omega_n^2 \quad (42)$$
$$\frac{d_\theta}{dt} = \frac{d_k}{dt} = -\gamma e \frac{\partial e}{\partial k} = -\gamma e \frac{\partial y}{\partial k} \quad (43)$$

In conclusion, the adjustment for the controller parameters is:

$$\frac{dk_1(t)}{dt} = -\gamma \left(\frac{1}{p^2 + 2\xi\omega_n p + \omega_n^2} r(t) \right) e(t) \quad (44)$$
$$\frac{dk_2(t)}{dt} = \gamma \left(\frac{1}{p^2 + 2\xi\omega_n p + \omega_n^2} y(t) \right) e(t) \quad (45)$$
$$\frac{dk_3(t)}{dt} = \gamma \left(\frac{1}{p^2 + 2\xi\omega_n p + \omega_n^2} \dot{y(t)} \right) e(t) \quad (46)$$

After mathematical modeling the MIT rule, the simulation block diagram is given in the Fig. 9 below as we know 'p' is a differential operator:

Where, $K_1 = K_P, K_2 = K_I, K_3 = K_D$ of PID controller gains. And parameter $\alpha_1$is introduced in the adaptation gainγ.

Assuming a critically damped second order system is chosen as reference model with damping ratio as 1 and natural frequency as 1000 whose transfer function is given by:

$$G_m(s) = \frac{y_m(s)}{r(s)} = \frac{1000000}{s^2 + 2000s + 1000000} \quad (47)$$

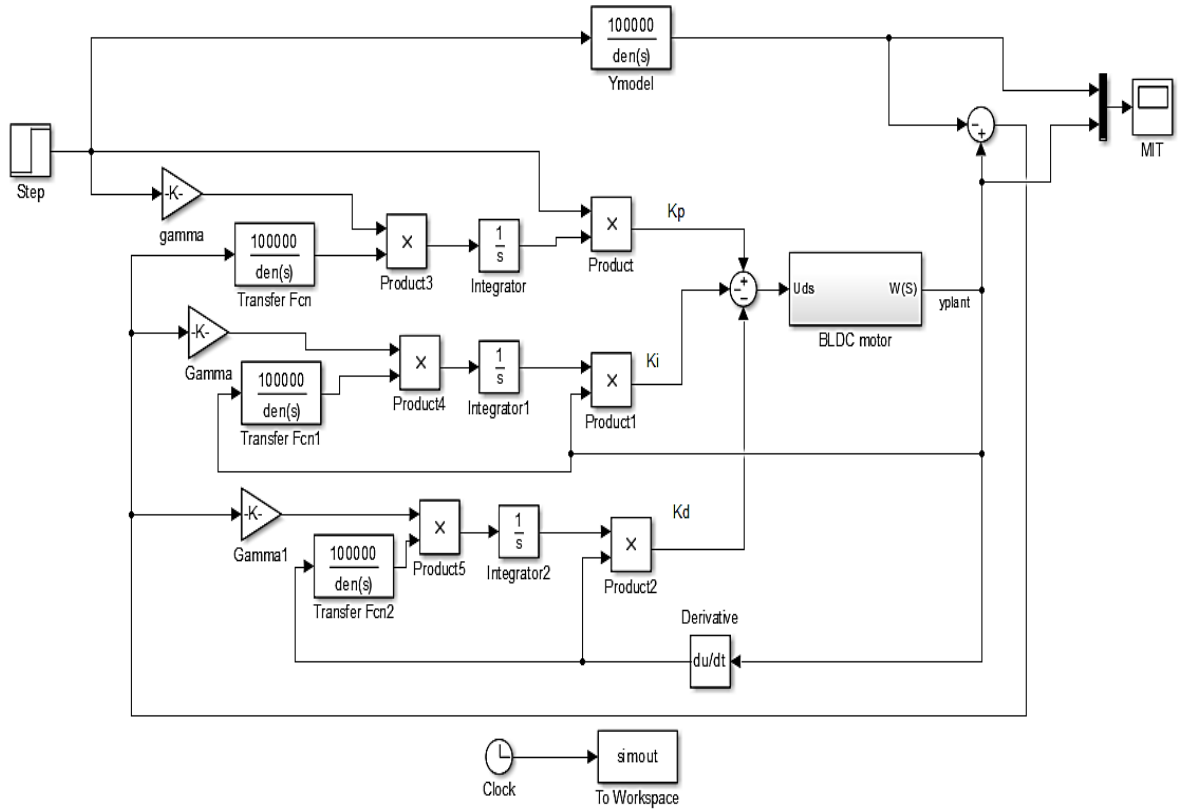

Figure 9: *MATLAB Simulink module of MIT rule.*

https://doi.org/10.46610/JOIIS.2021.v06i01.001

The above MIT design is designed with a reference signal of step input to analysis the model how much is tracking the plant signal with estimated parameter as.

Design of MRAC using Modified MIT Rule

Normalization can be used to protect against dependence on the signal amplitudes.

With$\varphi = \frac{\partial e}{\partial \Theta} = \frac{\partial y}{\partial \Theta} = \frac{\partial y}{\partial k}$ (48)

Where; φNormalization constant,

The MIT rule can be written as:

$$\frac{d\Theta}{dt} = \frac{dk}{dt} = -\gamma\varphi e \quad (49)$$

The normalized MIT rule is then become:

$$\frac{d\Theta}{dt} = \frac{dk}{dt} = \frac{-\gamma\varphi e}{\alpha^2 + \varphi^T\varphi} \quad (50)$$

From equation (37) we can get the close loop transfer function with differential operator 'p' becomes:

$$y(t) = \frac{\alpha_1 K_1 r(t)}{p^2 + (\alpha_2 + \alpha_1 k_3)p + \alpha_3 + \alpha_1 k_2} \quad (51)$$

The sensitivity derivatives are obtained by taking the partial derivatives of the error and considering the controller parameters and as we know $\frac{\partial e}{\partial \Theta} = \frac{\partial y}{\partial k} = \frac{\partial y}{\partial \Theta}$.

Hence:

$$\frac{\partial e}{\partial k_1} = \gamma\left(\frac{1}{p^2 + 2\xi\omega_n p + \omega_n^2} r(t)\right) e(t) \cong y_m = G_m r \quad (52)$$

$$\frac{\partial e}{\partial k_2} = \gamma\left(\frac{1}{p^2 + 2\xi\omega_n p + \omega_n^2} y(t)\right) e(t) = -G_m y \quad (53)$$

$$\frac{\partial e}{\partial k_3} = \gamma\left(\frac{1}{p^2 + 2\xi\omega_n p + \omega_n^2} \dot{y}(t)\right) e(t) = -G_m \dot{y} \quad (54)$$

In conclusion, with approximation and the adjustment controller parameters are:

$$\frac{dk_1}{dt} = \frac{-\gamma y_m e}{\alpha + y_m^2}$$

$$\frac{dk_2}{dt} = \frac{\gamma G_m y e}{\alpha + (G_m y)^2} \quad (55)$$

$$\frac{dk_3}{dt} = \frac{\gamma G_m \dot{y} e}{\alpha + (G_m \dot{y})^2} \quad (56)$$

Therefore, the modified MIT rule Simulink block diagram is given in Fig. 10 below as the derived mathematical equation of the modified MIT rule with $K_P, K_I \; and \; K_D$values of $K_1, K_2 \; and \; K_3$ respectively.

https://doi.org/10.46610/JOIIS.2021.v06i01.001

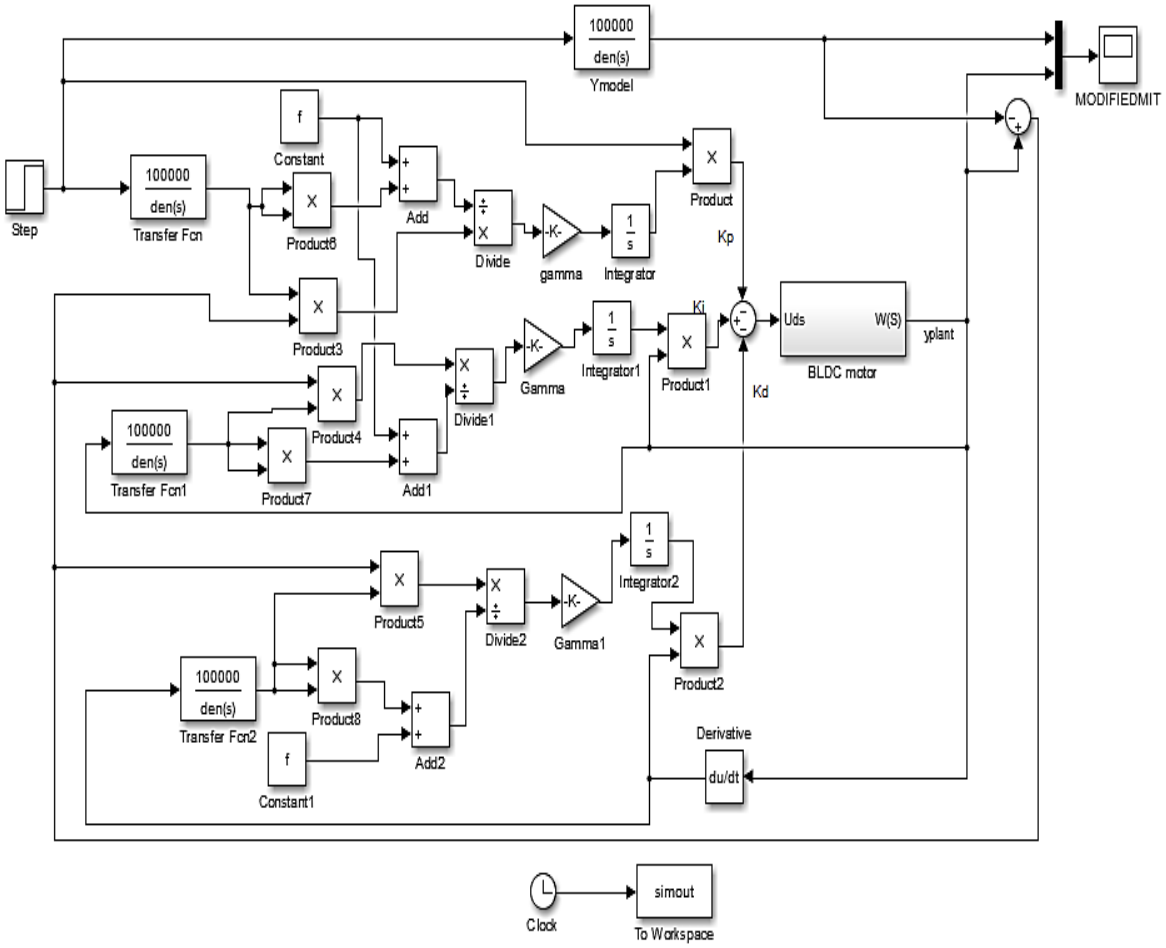

Figure 10: *Simulink model of Modified MIT rule.*

MRAC with Lyapunov Stability Method

The Lyapunov function is described $v(e, \theta_1, \theta_2, \theta_3)$. This function should be positive semi definite and is zero when error is zero. For stability according to Lyapunov theorem the derivative $^{dv}/_{dt}$ must be negative. The derivative$^{dv}/_{dt}$ requires the values of $d\theta 1/dt, d\theta 2/dt$ and $d\theta 3/dt$. If the parameters are updated then so $^{dv}/_{dt}$ is negative semi definite. This shows that V(t) = V(0) and e, θ1, θ2 and θ3 must be bounded and also Lyapunov removes the filter of MIT rule and uses the simplified mathematical model which is given below after we derived using Lyapunov rule of the given form. The Lyapunov Function is taken as:

$$v(e, \theta_1, \theta_2, \theta_3) = v(e, k_1, k_2, k_3) \qquad (57)$$

$$v(e, k_1, k_2, k_3) = {}^{1}/_{2}\,(e^2 + \frac{1}{by}(bk_3 + a - a_m)^2 + \frac{1}{by}(bk_2 + a - a_m)^2 + \frac{1}{by}(bk_1 - b_m)^2) \qquad (58)$$

$$\frac{dk(t)}{dt} = -\gamma\left(\frac{p}{p+4}r(t)\right)e(t) \cong -\gamma\big(r(t)\big)e(t) \qquad (59)$$

According to Lyapunov, the system is said to be stable when $^{dv}/_{dt}$ is negative definite. So, in order to make the system stable the parameters are updated as:

$$\frac{dk_1(t)}{dt} = -\gamma\big(r(t)\big)e(t) \qquad (60)$$

https://doi.org/10.46610/JOIIS.2021.v06i01.001

$$\frac{dk_2(t)}{dt} = \gamma\big(y(t)\big)e(t) \quad (61)$$

$$\frac{dk_3(t)}{dt} = \gamma\big(\dot{y(t)}\big)e(t) \quad (62)$$

Therefore, The Lyapunov Simulink block diagram accordingly is given in Fig. 11.

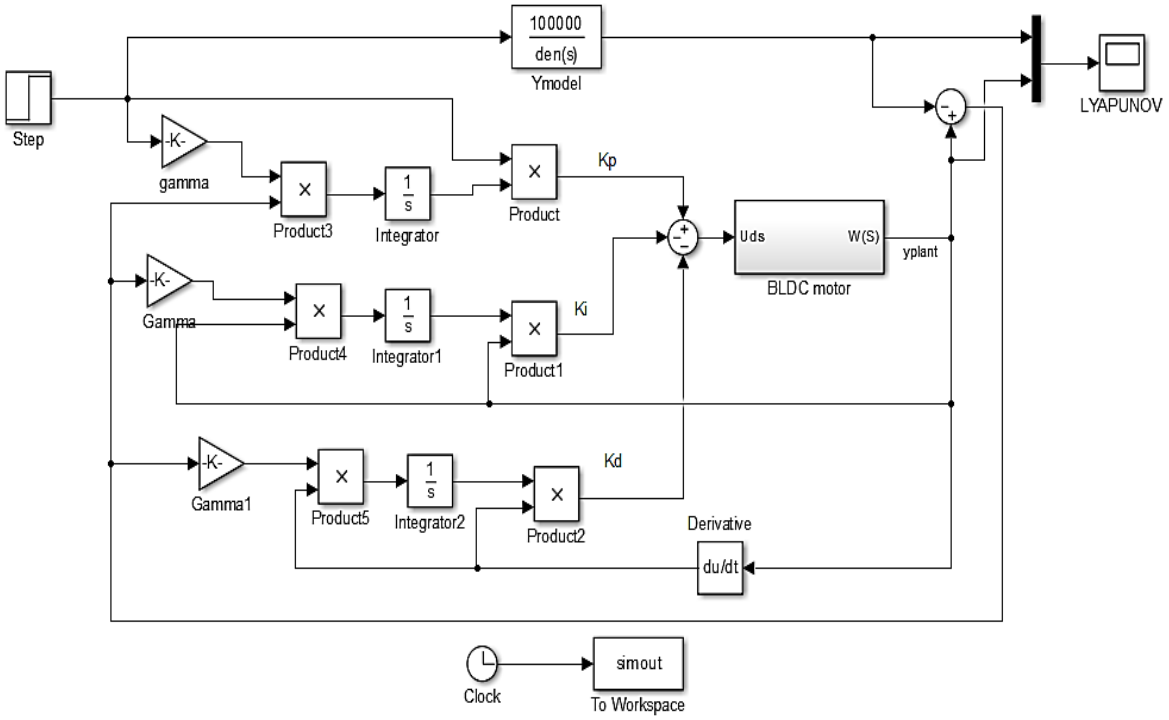

Figure 11: *System block diagram of Lyapunov method.*

Applying of Fuzzy Logic Controller

Atypical fuzzy-control system is composed of a fuzzy controller and a plant. The fuzzy controller involves four components: fuzzification, knowledge database (including the database and rule base), fuzzy inference and defuzzification. Fundamentally, fuzzy controls can reflect human reasoning. It is an intelligent control method that is independent of the precise mathematical model of the controlled object Speed Control Using FLC.

In the case of motor speed control, the two needed input variables for FLC is the motor speed error (E) and its derivative, which represents the change of speed error (CE). Whereas, the controller output is the change in frequency (CF) of the voltage supply fed to motor. Change of speed error could be given as follows:

$$E = V_{ref} - V_{act} \quad (63)$$

$$CE = \frac{dE}{dt} \quad (64)$$

Where$V_{ref}$the desired motor speed and $V_{act}$is the measured motor speed which is given in Fig. 12.

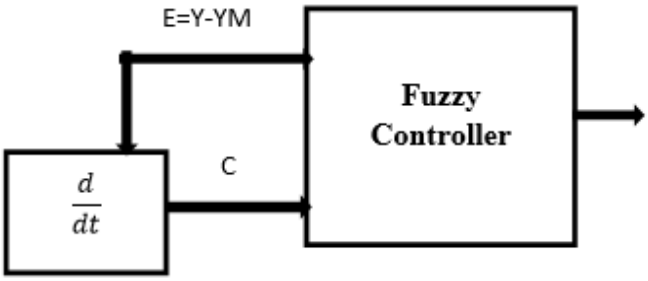

Figure 12: *Block diagram of Fuzzy control system.*

https://doi.org/10.46610/JOIIS.2021.v06i01.001

Rule Base

There are 7 speed error variables and 7 changes in speed error variables are taken, so there are total 49 rules which governed the decision are making mechanism. The foremost vital step in planning fluffy framework is the plan of the run the show base. It consists of a number of fuzzy IF-THEN rules that define the behavior of the system. The Table 2 below shows the corresponding rule base table for the proposed fuzzy control system. The top row of the matrix indicates the fuzzy sets of the error variable E and the left column indicates the change in error variable CE and the output variable U is shown in the body of the matrix.

Table 2: *Rule base table.*

CE / E	NL	NM	NS	ZE	PS	PM	PL
NL	NL	NL	NLM	NM	NMS	NS	ZE
NM	NL	NLM	NM	NMS	NS	ZE	PS
NS	NLM	NM	NMS	NS	ZE	PS	PMS
ZE	NM	NMS	NS	ZE	PS	PMS	PM
PS	NMS	NS	ZE	PS	PMS	PM	PLM
PM	NS	ZE	PS	PMS	PM	PLM	PL
PL	ZE	PS	PMS	PM	PLM	PL	PL

Method to mimic the fluffy controller in MATLAB:

- First rule have to be coded and written in m-file and saved with FIS extension.
- Then the FIS editor will be opened by typing fuzzy in the command window.
- Then the specified FIS record should be imported by browsing.
- After the loading of FIS file the controller is ready to be operated. All the above procedures are simulated with figure below.

After giving the fuzzy command in the command window, then Fig. 13 FIS Editor window will be opened as shown below.

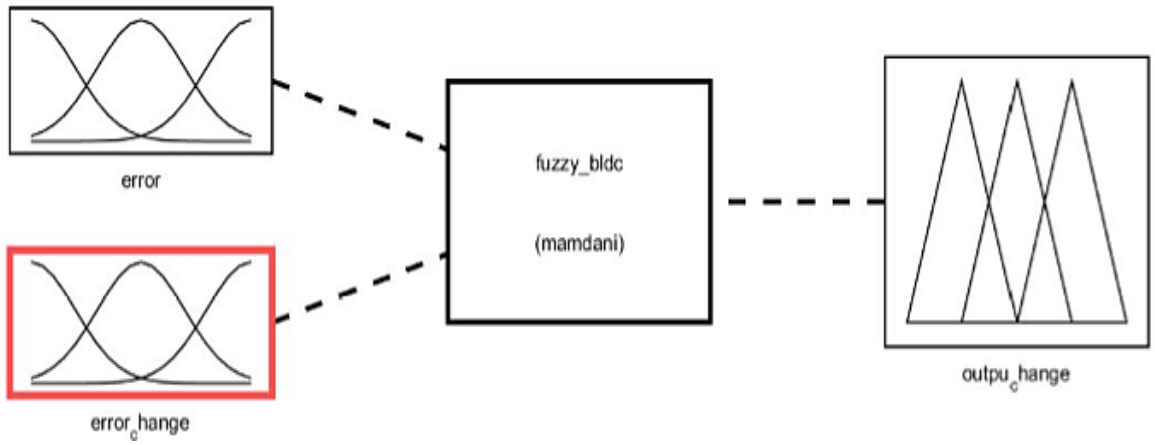

Figure 13: *FIS Editor Window.*

Then after importing the FIS file FIS Editor Rule's window will be opened as shown in Fig. 14 below with input of error and change of error.

https://doi.org/10.46610/JOIIS.2021.v06i01.001

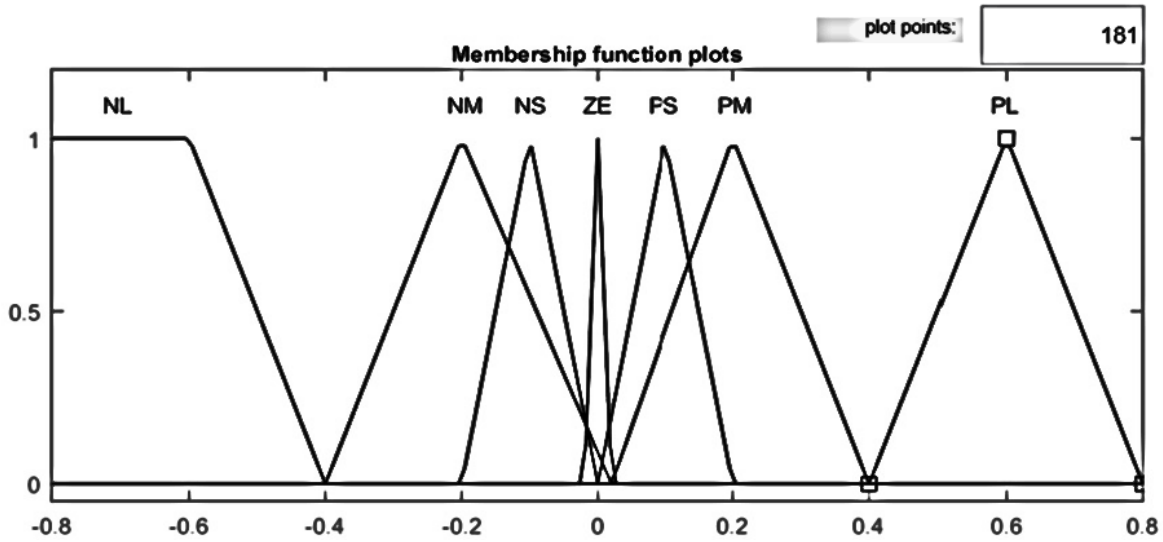

Figure 14: *Membership function plots of input error and change of error.*

Similarly, the membership function of output change can also be seen below in Fig. 15.

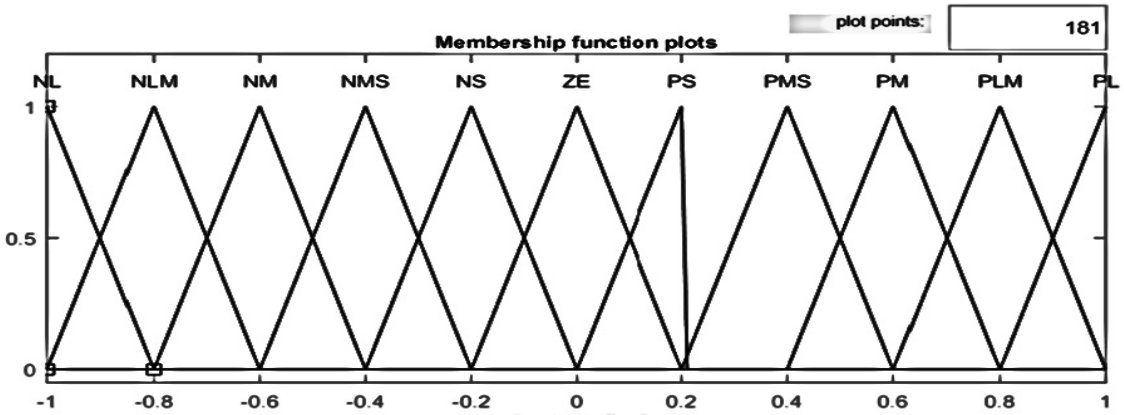

Figure 15: *Membership Function of output change.*

- In the FIS Editor Window rules view window, by clicking on view, rules and surface can also be seen below in Fig. 16 and 17.

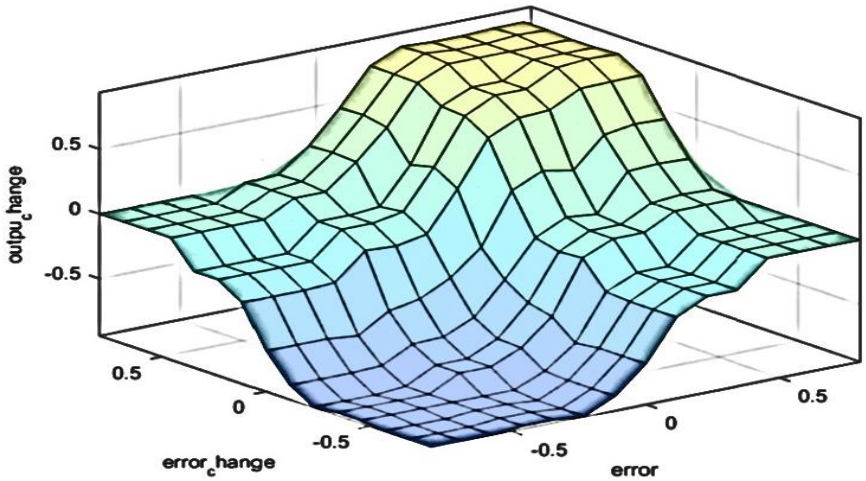

Figure 16: *3-dimensional view of control surface.*

https://doi.org/10.46610/JOIIS.2021.v06i01.001

Rule View of the control also can be shown Fig. 17 below at a given value of error and change of error with relative change of output.

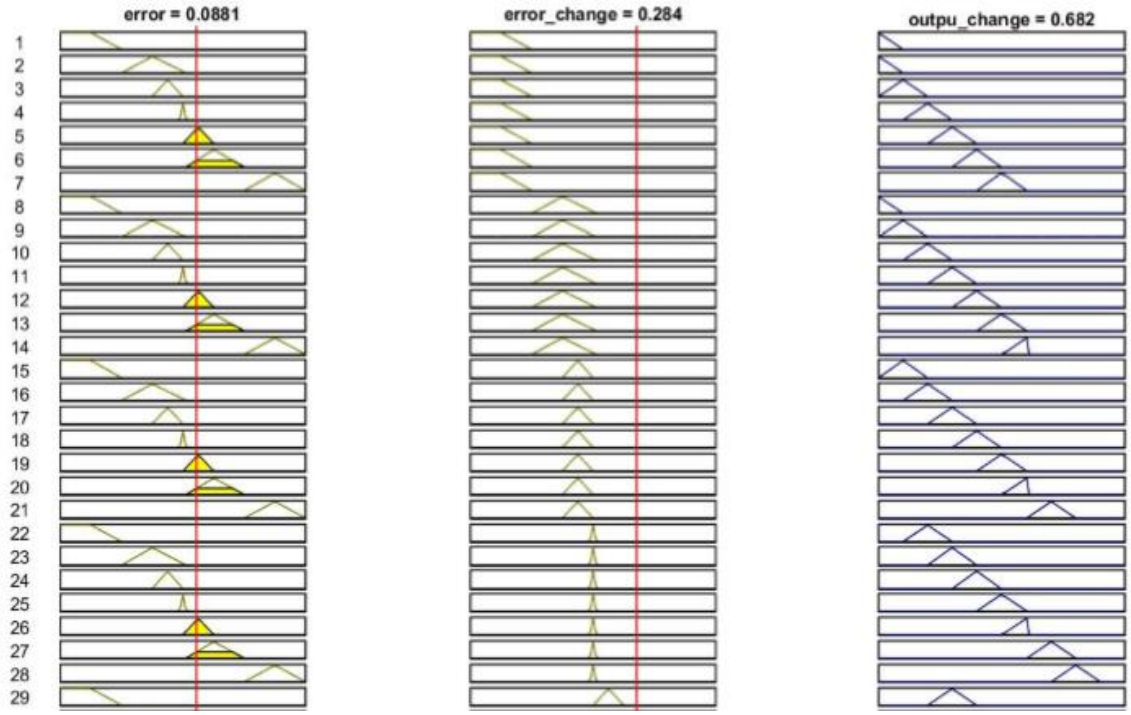

Figure 17: *Rule Viewer with input E= 0.0881 and CE=0.264, Change of control=0.682.*

PROPOSED CONTROLLER DESIGN

Fig. 18 given below shows the proposed system design of the BLDC motor and Fig. 19 below shows the Simulink diagram. The controller generates the control signal based on the Fuzzy based model reference adaptive control law which is used for speed regulation and adapting purpose. Model reference adaptive controls are in general considered being applicable to plants that are mathematically understood and where the fuzzy system experienced human operators or behavioral learners are available. Then a controller is constructed assuming that the MRAC system approximately represents the true plant as well as the model.

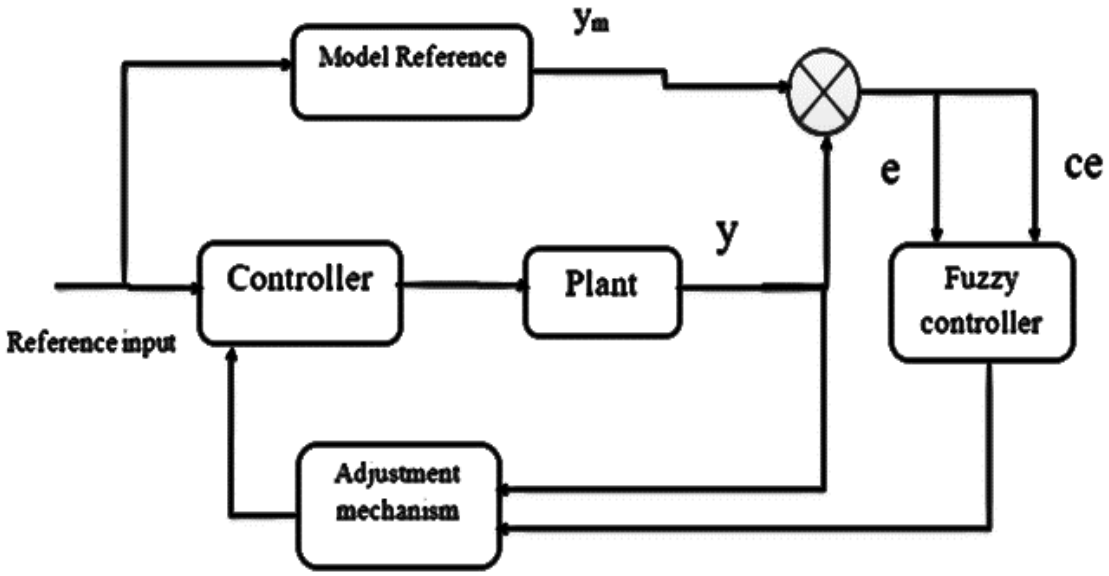

Figure 18: *Complete proposed System design.*

https://doi.org/10.46610/JOIIS.2021.v06i01.001

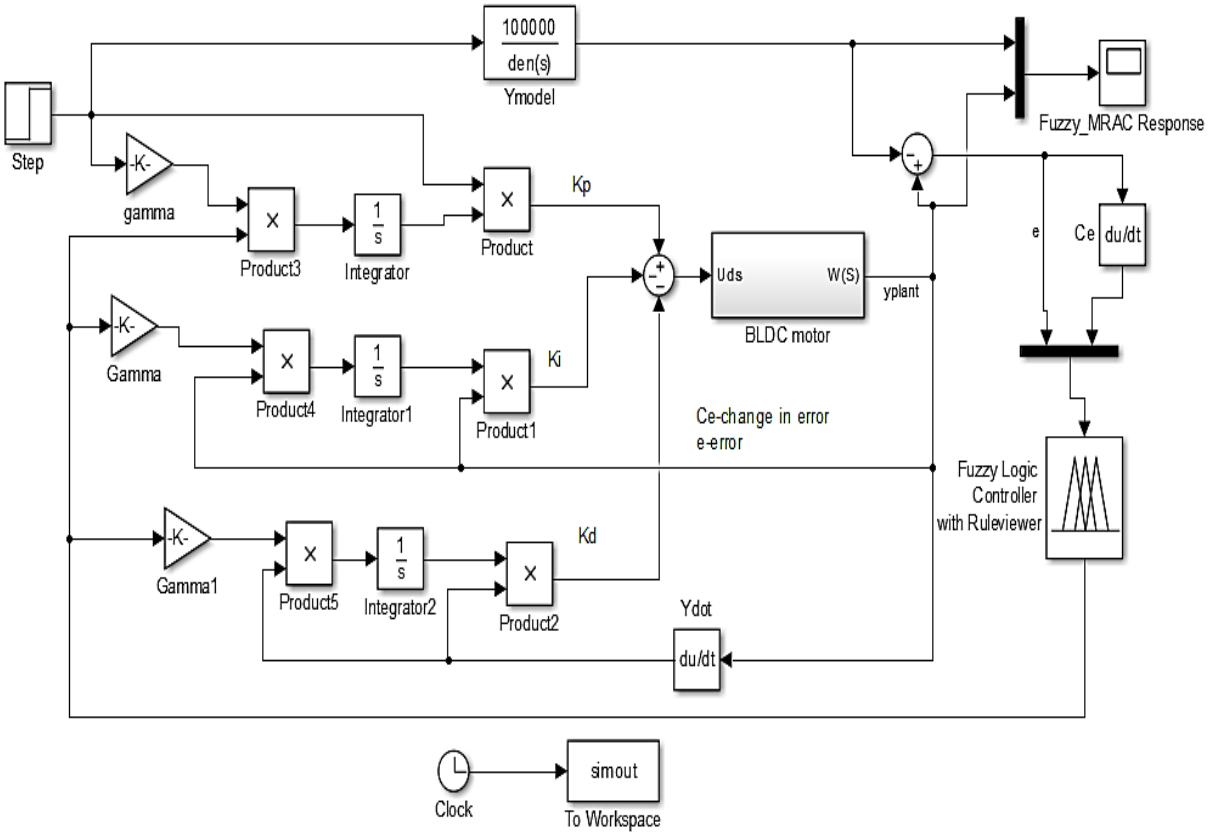

Figure 19: *Proposed System Simulink Block Diagram.*

RESULT AND DISCUSSION

A Brushless DC motor drive system was modeled. An adaptive controller with MIT rule and Lyapunov Stability Method with Fuzzy was intended and applied to the model and as compared with the results of the conventional PID and simple MRAS controller as well as open loop response. All the reenactments were carried out in MATLAB/ Simulink. Step input was given as the reference to study the response of controller with sudden load change.

Open Loop Response

The Open loop response of the plant is given in the Fig. 20 with Simulink model and the load response of the plant with load torque is given below to characterize how much the plant resists a load torque and a base for close loop response characterization property.

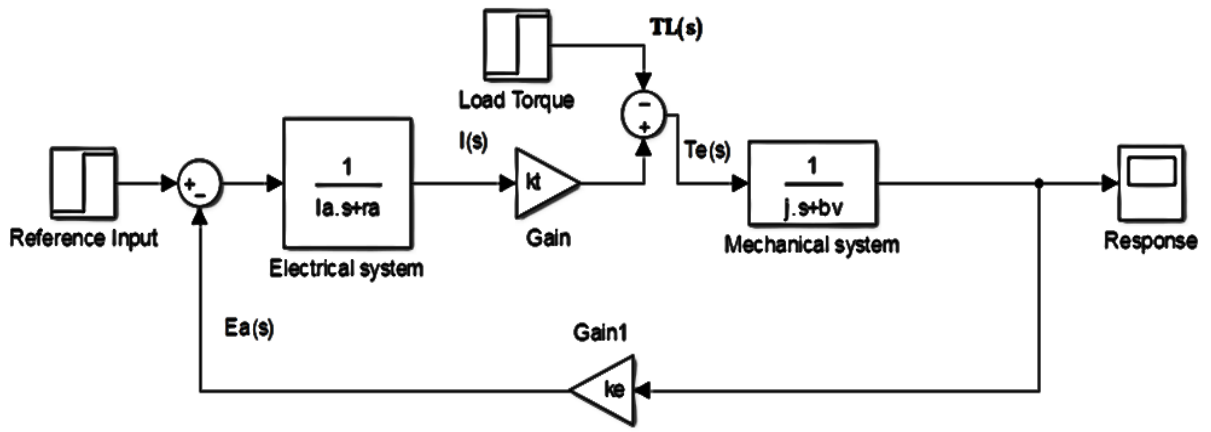

Figure 20: *Open loop Simulink model.*

e-ISSN: 2456-9860
Volume-6, Issue-1 (January-April, 2021)
https://doi.org/10.46610/JOIIS.2021.v06i01.001

Therefore, from the above Simulink model we have examined the open loop response with no load and with load condition and the load torque is varied from 100_300Nm and rated speed is 1500rpm is given for examination.

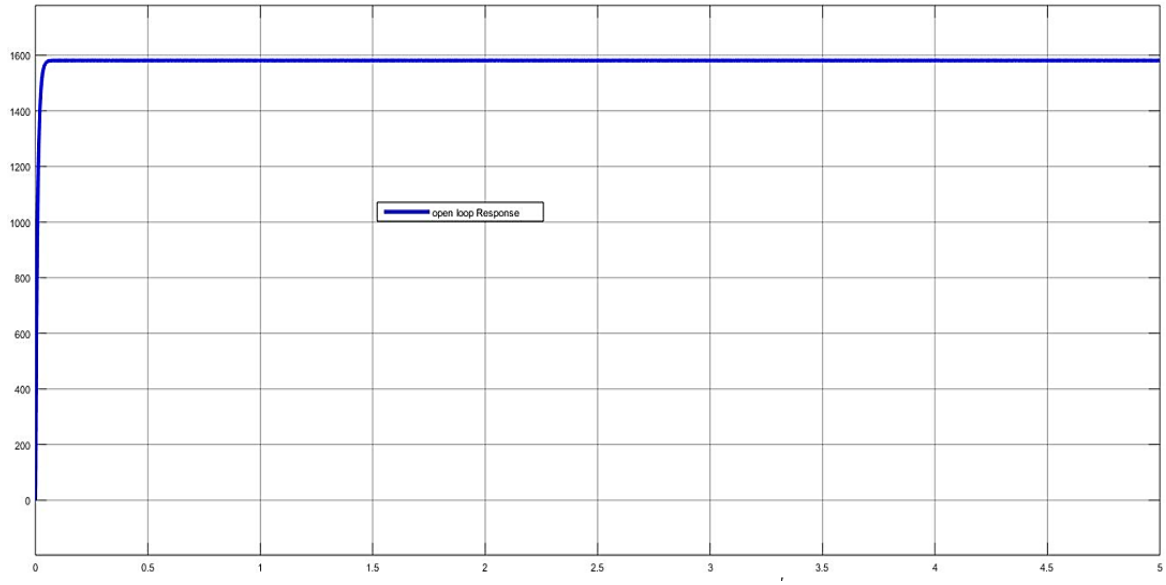

Figure 21: *No load Open loop response with no load.*

From the Fig. 21 above we noticed that the plant response with a percentage overshoot of 0.495%, Rise time of 19.253ms and settling time of 12.871ms to operate as open loop.

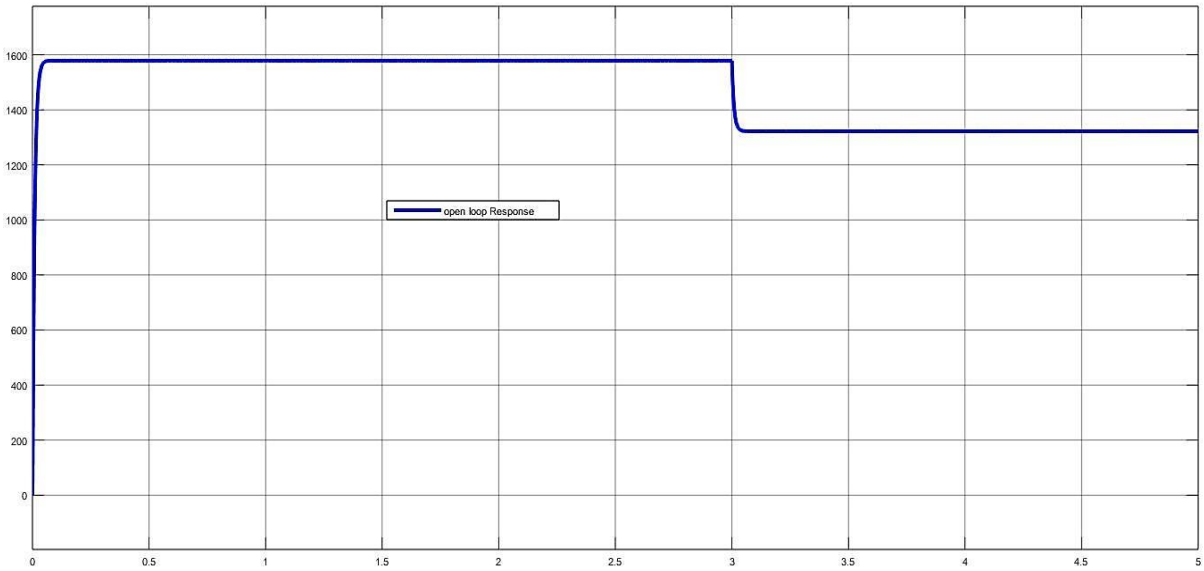

Figure 22: *Open loop Response with Load torque 300Nm response.*

From Fig. 22 open loop response Load torque 300Nm, we have observed that the plant never come to the original place after applied and continues where load torque applied and the plant response with open loop Rise time of 19.253ms, settling time of 12.871ms and with some increscent of a percentage overshoot 0.495% to operate as open loop with load torque of 300Nm at 3seconds.

Response of PID Controller

The controller parameters for the routine PID controller are found such that it ensures required following conjointly keeps up the

e-ISSN: 2456-9860
Volume-6, Issue-1 (January-April, 2021)
www.matjournals.com
https://doi.org/10.46610/JOIIS.2021.v06i01.001

solidness of the generally framework when compared to open circle reaction. Zeigler Nicholas strategy of tuning is utilized to discover the controller parameter which adapt with the consistent state blunder, overshoot and settling time prerequisites. The arranged controller parameters are kp =5.7748, ki=1605.29, kd=0.00468 for speed taking after execution. The step reactions of the customary PID controller for the framework with variety in speed from 1000 rpm to 1500 rpm and a stack torque of appraised 300Nm is connected as appeared underneath in Fig. 23 and 24 individually, tall overshoot up to 1200-2000 rpm is watched for the framework to maintain the working condition of the plant. In arrange to diminish overshoot the controller with Show Reference Versatile control strategy is outlined below.

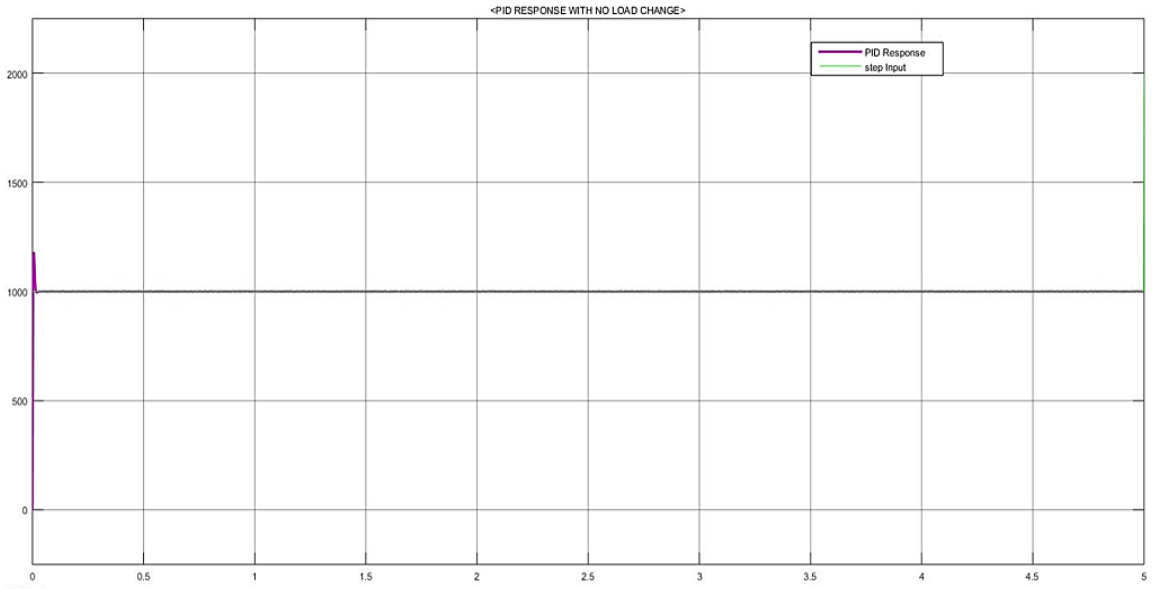

Figure 23: *No Load Response of PID controller at 1000rpm.*

At rated speed with no load response of the plant, the close loop controller response of a conventional PID controller applied on the plant responses with a settling time of 12.284ms, Rise time of 2.552ms and a percentage over shoot of 18.452%.

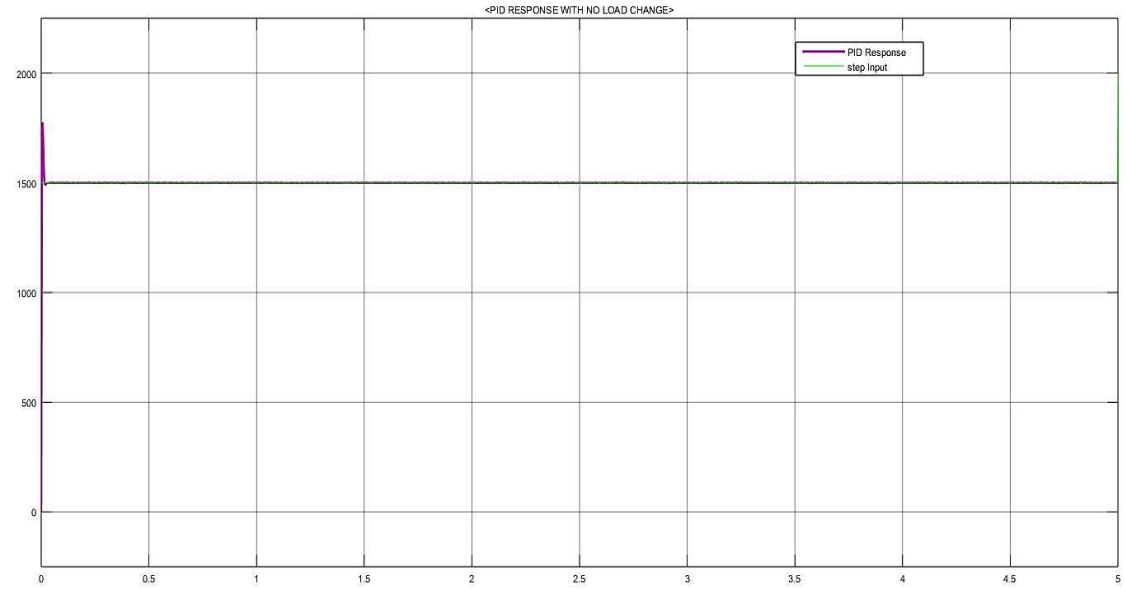

Figure 24: *No Load Response of PID controller at 1500rpm.*

e-ISSN: 2456-9860
Volume-6, Issue-1 (January-April, 2021)
https://doi.org/10.46610/JOIIS.2021.v06i01.001

At rated speed with no load response of the plant increases, the close loop controller response of a conventional PID controller applied on the plant responses also increases in some condition with a settling time of 12.131ms and decreases with some condition of Rise time of 2.552ms and a constant percentage over shoot of 18.452% is observed with no load condition which indicates that changing rated input speed does not have fundamental change so we have been considered only on load change condition.

Response of PID Controller with Sudden Load Change

In order to authenticate the performance of the proposed controller setup is subjected to the different test cases, like sudden changes in load and sudden changes in speed. The results of which are presented here in Fig. 25 at 1000rpm and 1500rpm motor operation is in order to validate the model with a sudden load change applied at 3 seconds with rated speed of load torque. Initially the motor is run at no load and then the speed curve points to the no load operation.

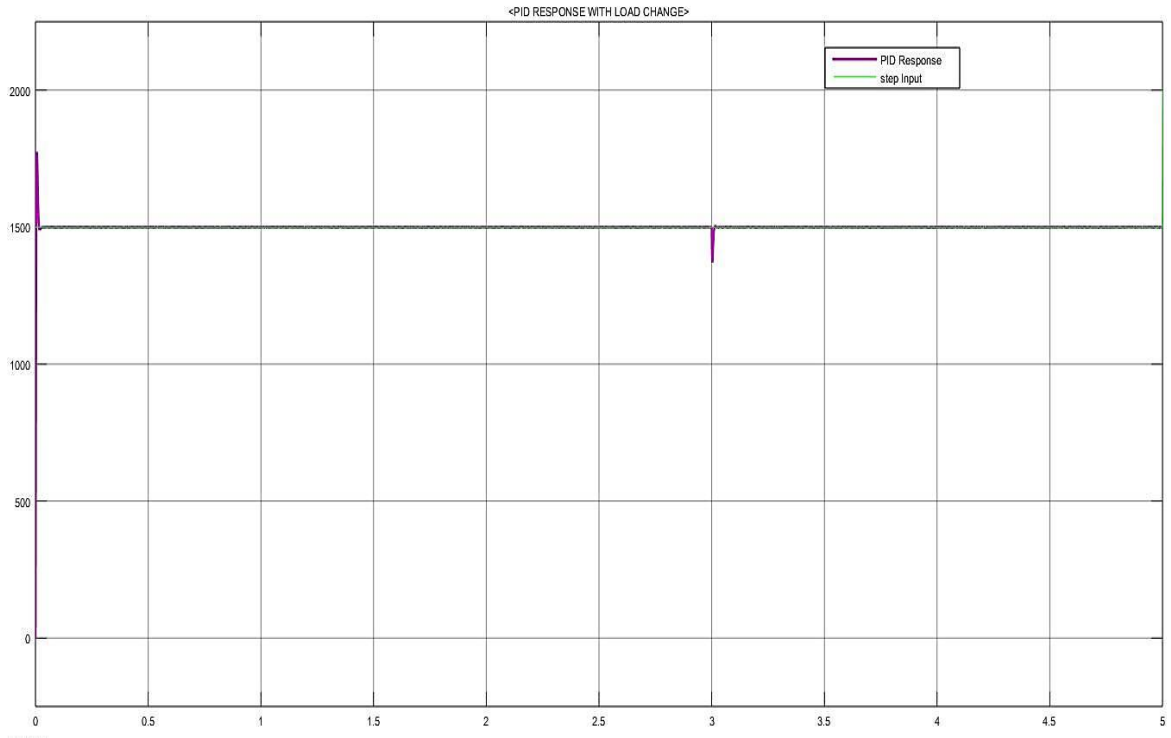

Figure 25: *Response of PID controller at 1500rpm with sudden load change.*

Response of Model Reference Adaptive Control

The Show Reference Versatile controller is planned as talked about within the over segments. Mistake between the reference speed and genuine speed is constrained to zero utilizing adjustment component. The reactions of the framework when MRAC with MIT, adjusted MIT run the show and Lyapunov solidness strategy is connected with variety of speed from 1000 rpm to 1500 rpm is appeared in Fig. 26 given underneath, For Versatile controller with MIT run the show we will see that the unsettling influences and overshoot are impressively decreased, hence decreasing the unfaltering state mistake and settling time. But we have same impressive overshoot.

No Load Response of Model Reference Adaptive Control

The following output shows the no load response of a model response adaptive controller with characteristics compression of steady state response.

e-ISSN: 2456-9860
Volume-6, Issue-1 (January-April, 2021)
www.matjournals.com
https://doi.org/10.46610/JOIIS.2021.v06i01.001

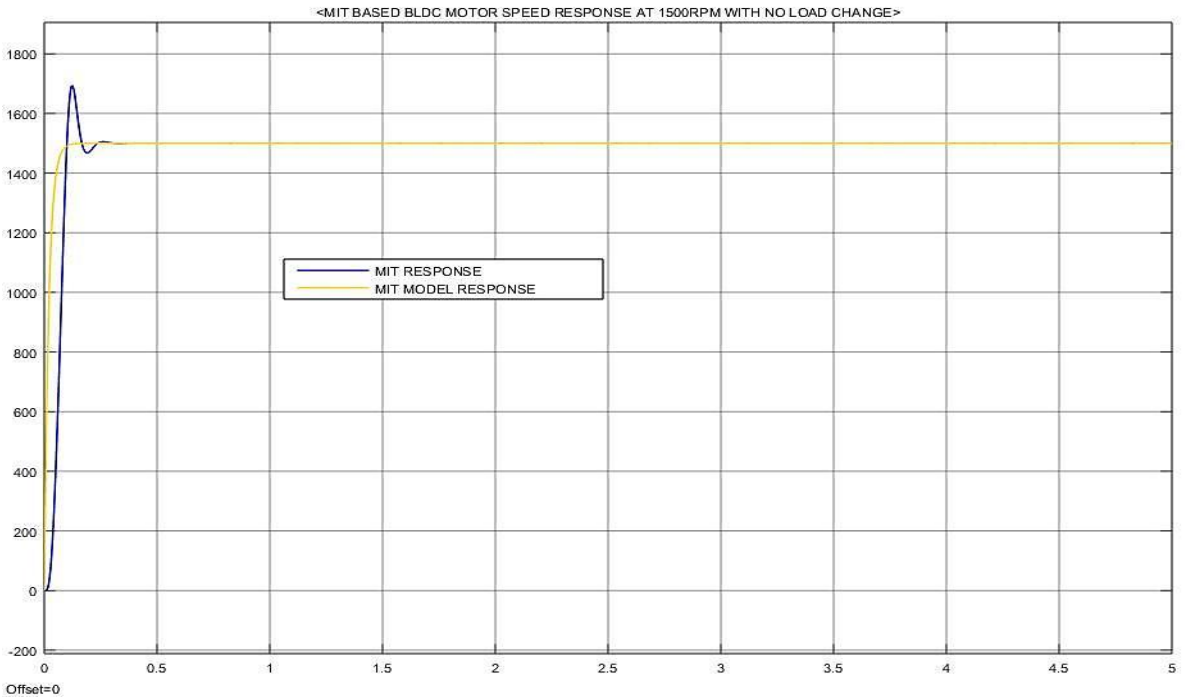

Figure 26: *Response of Model Reference Adaptive Controller with MIT rule at 1500rpm.*

From the response graph we have observed that the close loop response of the plant with model reference adaptive control is have some considerable change compared to with conventional PID controller with performance characteristics response of robustness hence the Rise time is 56.63ms, Settling time 0.4580s and a percentage overshoot of 13.0687% is observed.

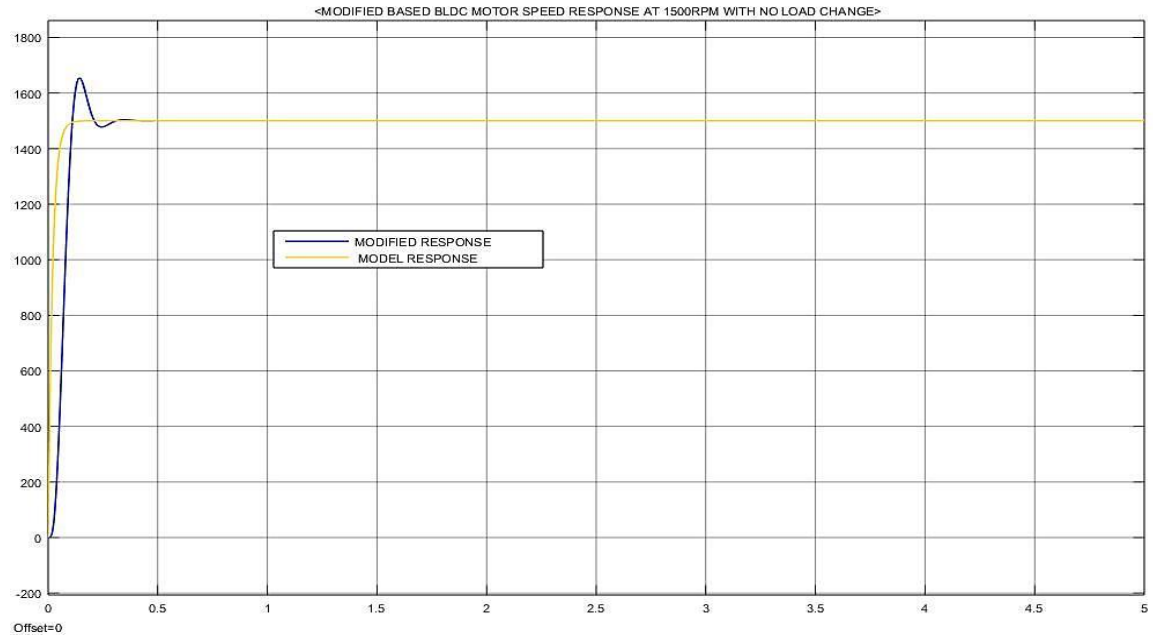

Figure 27: *Response of Model Reference Adaptive controller with modified MIT rule at 1500rpm.*

From the response graph of Fig. 27 we have observed that the close loop response of the plant with model reference adaptive control with Modified MIT rule is have some considerable change compared to with MIT rule controller with performance

e-ISSN: 2456-9860
Volume-6, Issue-1 (January-April, 2021)
https://doi.org/10.46610/JOIIS.2021.v06i01.001

characteristics response of robustness and the Rise time is 63.039ms,Settling time 0.485s and a percentage overshoot of 10.556% is observed witch is the Modified MIT rule have the ability to reduce the noise and some offset value or an overshoot compered to MIT rule.

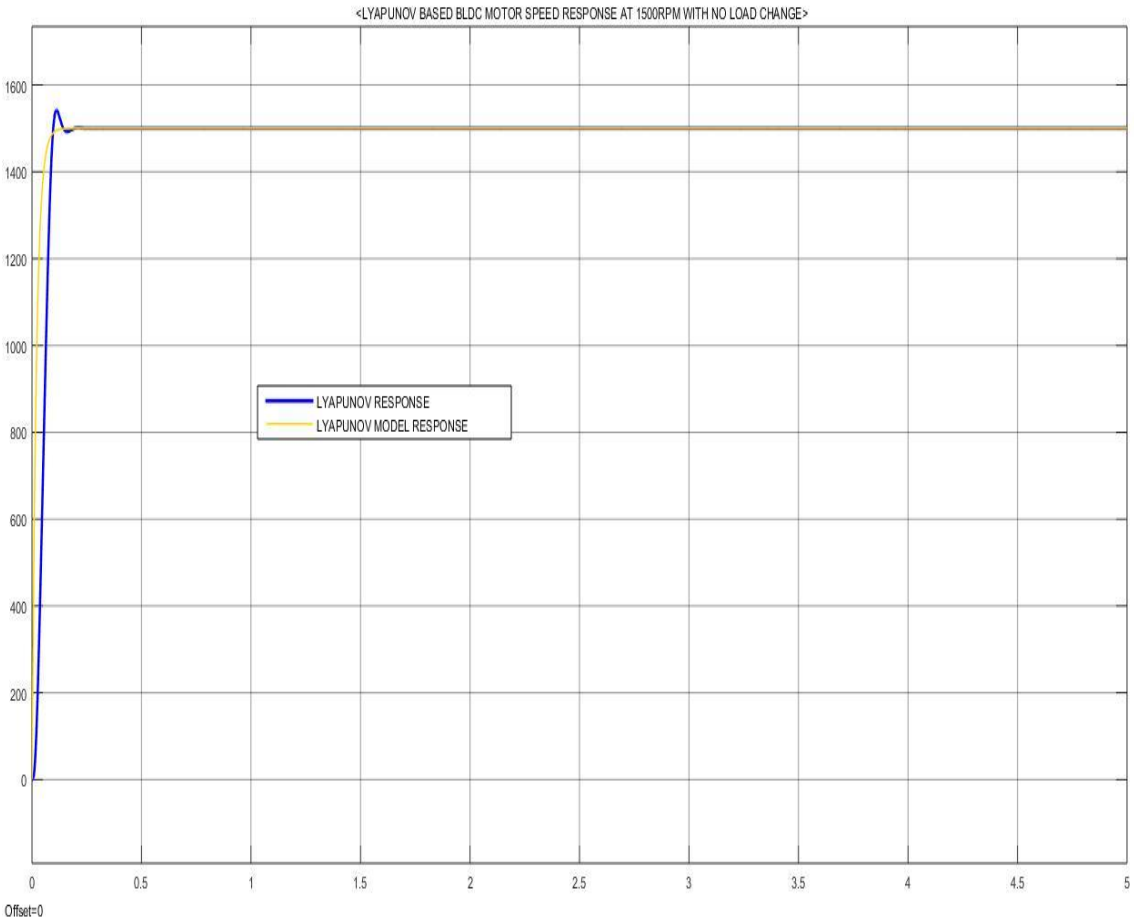

Figure 28:.*Response of Model reference Adaptive controller with Lyapunov Stability method at 1500rpm.*

From the above Lyapunov stability method response of close loop control system of Fig. 28, we have observed that the response of the plant is stable and almost adapting the model response and responding a stable response of the characteristics of robustness compared to the two-model reference adaptive controller and the Rise Time is 59.612ms, settling time 0.195s and a percentage overshoot of 2.577% is observed at no load condition.

Response of Model Reference Adaptive Control with Sudden Load Change

In order to validate the performance of the proposed controller setup is subjected to different test cases, like sudden change in load and sudden change in speed as we said before. The results of which are presented here in Fig. 29 below at 1000rpm and 1500rpm motor operation. In order to validate the model at a sudden load change is applied at 3.0seconds. Initially the motor is run at no load and then the speed curve points to the no load operation at the applied time of load.

e-ISSN: 2456-9860
Volume-6, Issue-1 (January-April, 2021)
www.matjournals.com
https://doi.org/10.46610/JOIIS.2021.v06i01.001

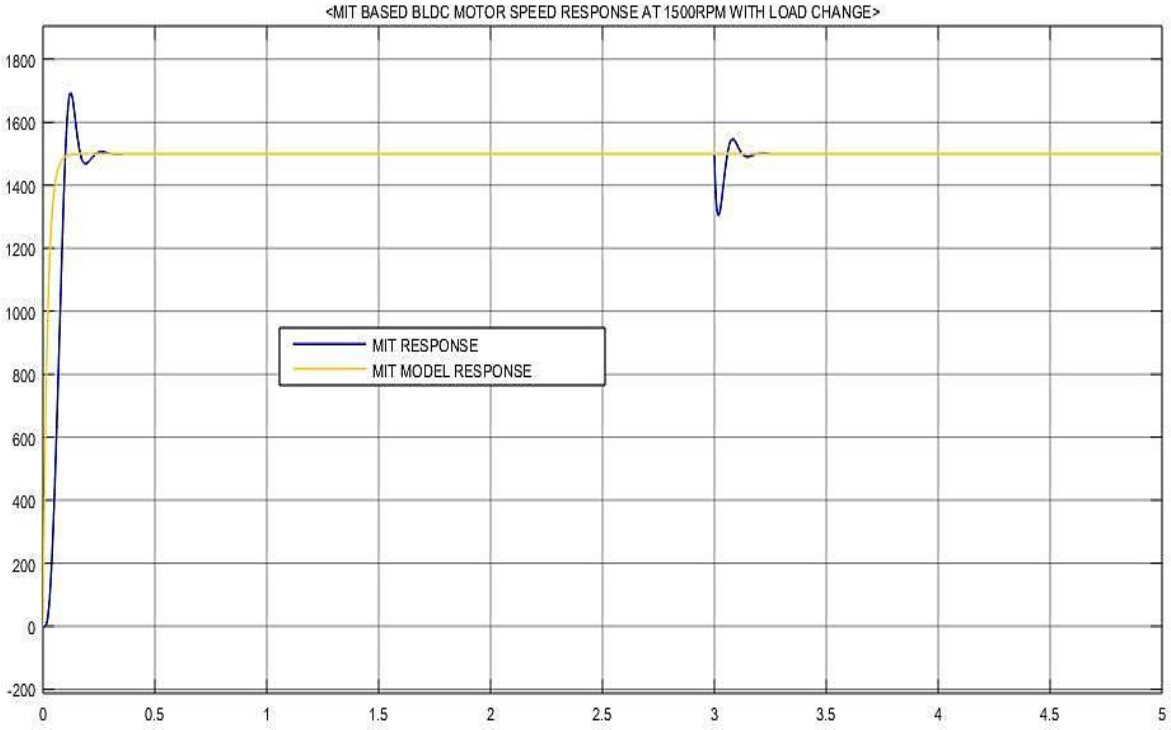

Figure 29: *MIT rule sudden load change at 1500rpm and 300Nm.*

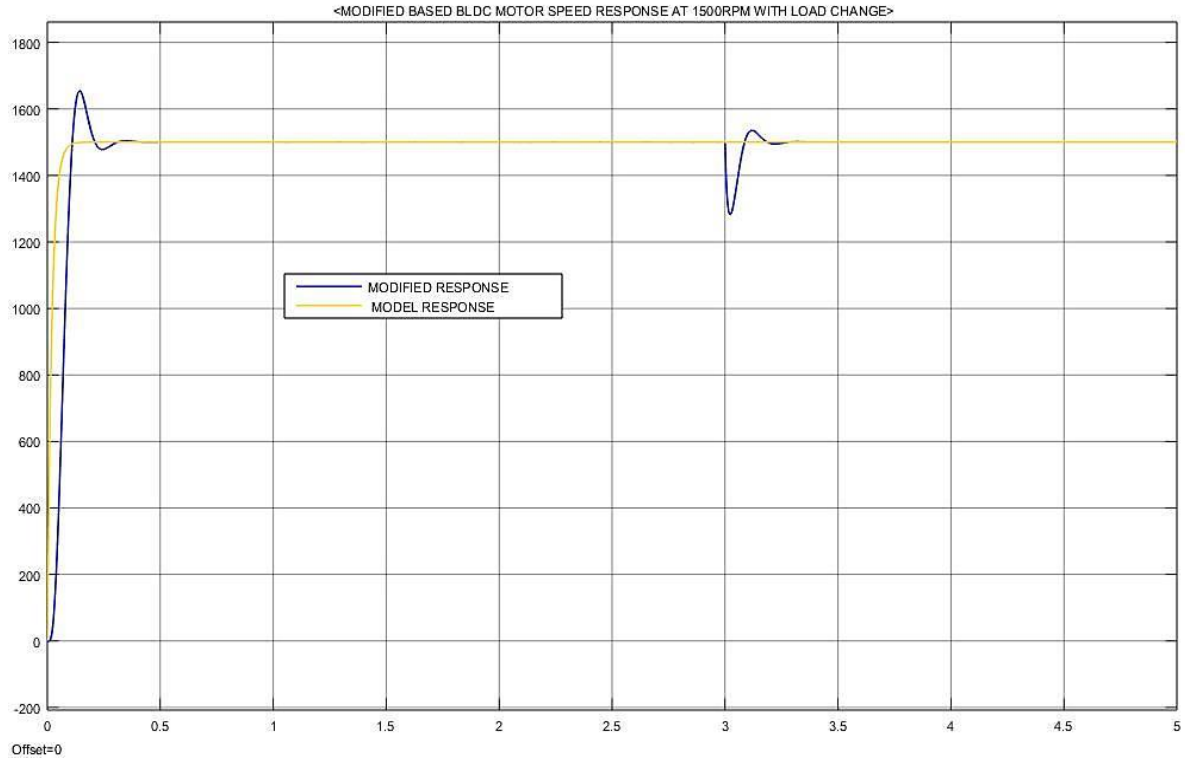

Figure 30: *Modified MIT rule sudden load change at 1500rpm and 300Nm.*

Lyapunov Stability Method Sudden Load Change

As explained above sudden load change in the plant response at rated speed of the plant is given below in Fig. 30, 31 and 32 with different input speed of the plant and a rated torque with rated speed respectively.

e-ISSN: 2456-9860
Volume-6, Issue-1 (January-April, 2021)
www.matjournals.com
https://doi.org/10.46610/JOIIS.2021.v06i01.001

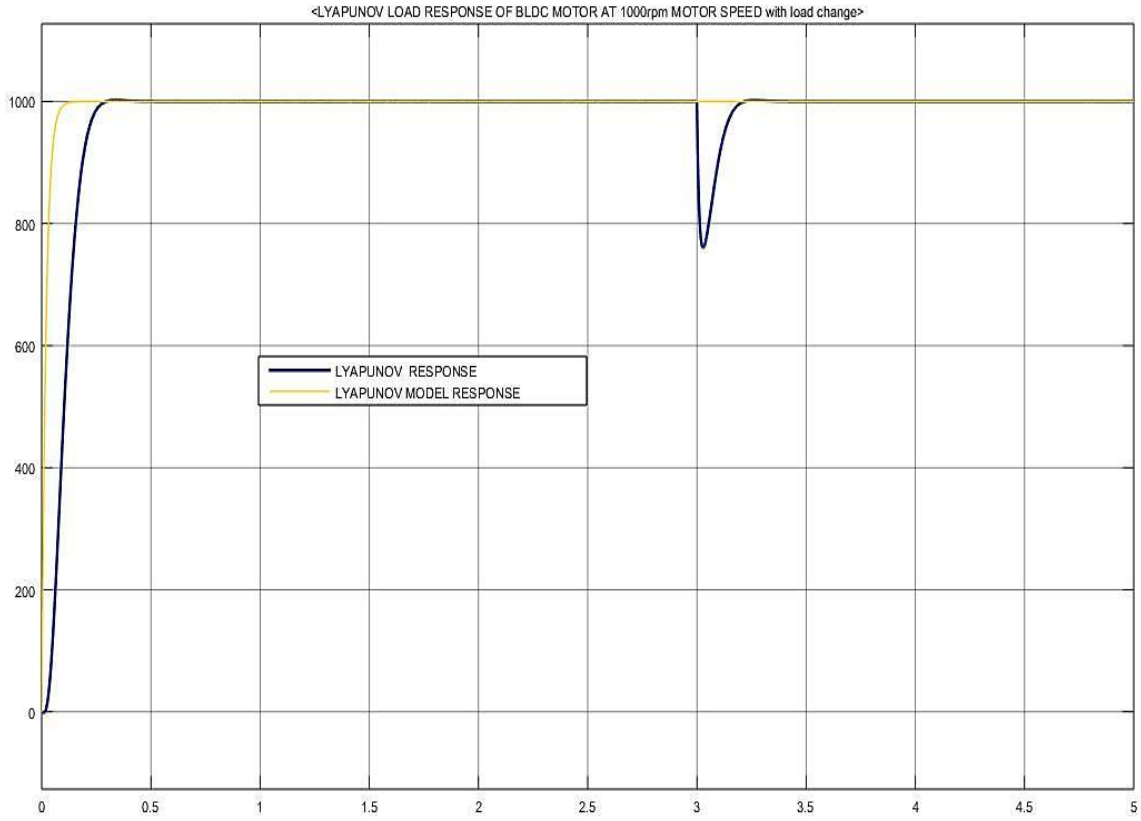

Figure 31:.*Lyapunov stability method sudden load change at 1000rpm and 300Nm Load.*

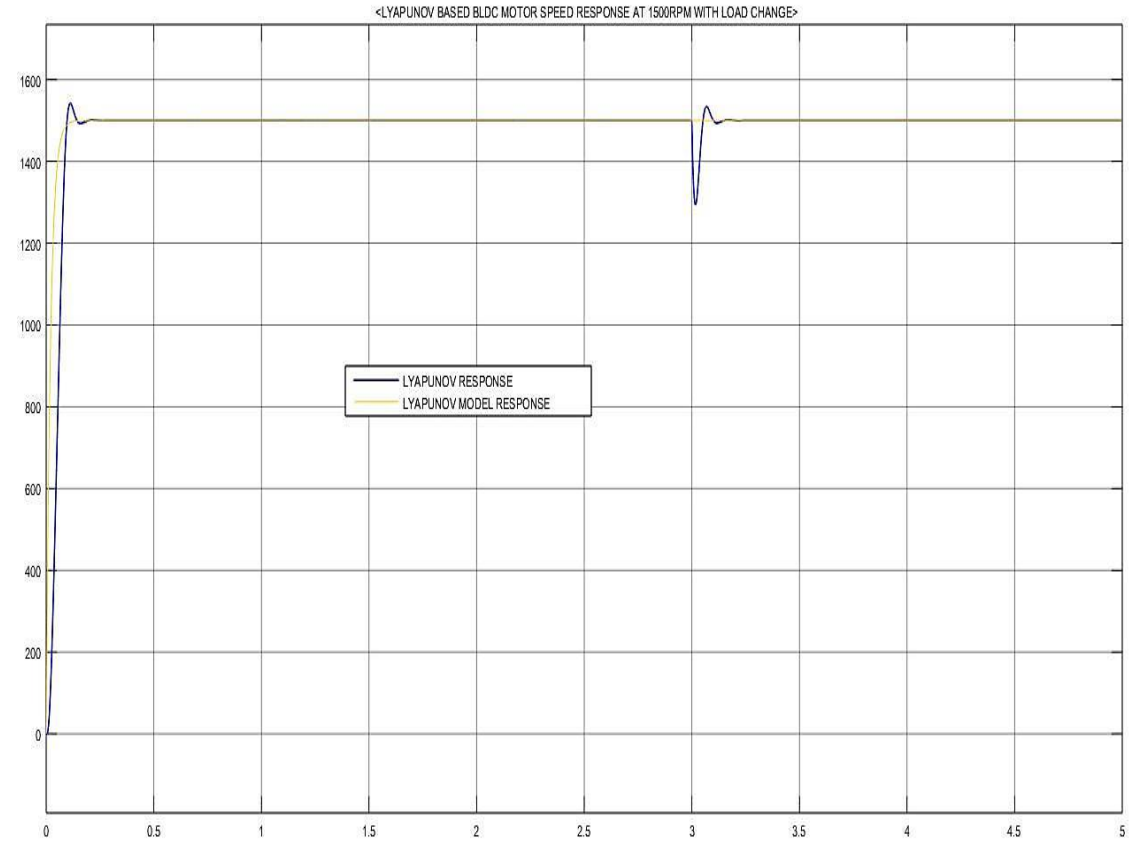

Figure 32: *Lyapunov stability method sudden load change at 1500rpm and 300Nm Load.*

e-ISSN: 2456-9860
Volume-6, Issue-1 (January-April, 2021)
https://doi.org/10.46610/JOIIS.2021.v06i01.001

Lyapunov Stability Method Sudden Load Change Gain and Error Response

The effect of the load change in the motor on the performance of the controllers was studied by changing the rated speed from 1000rpm to 1500rpm. The response of the Gain and Errors is shown in Figures given below Fig. 33 and 34 and Fig. 35 and 36 respectively.

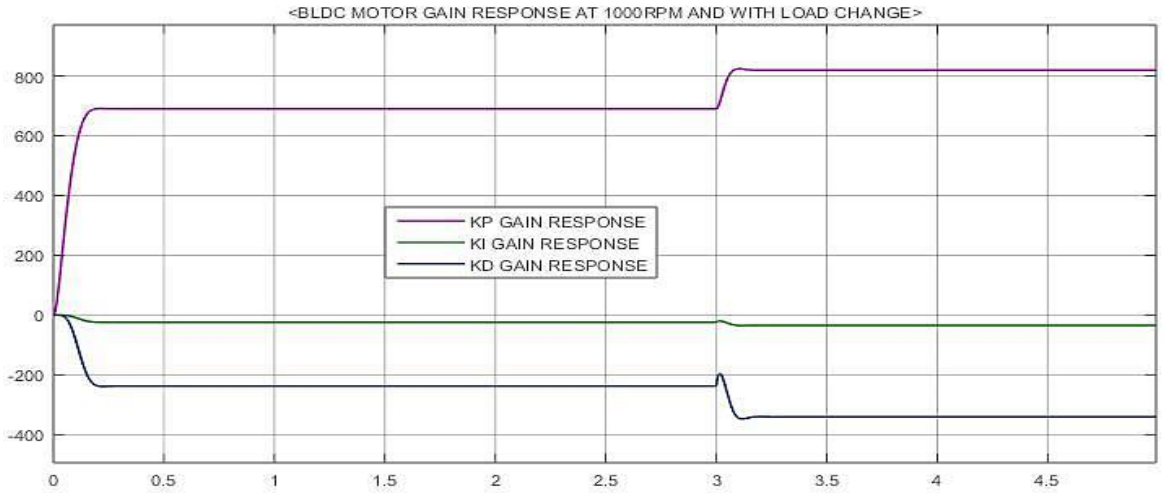

***Figure 33:**.Lyapunov stability method sudden load change Gain response at 1000rpm.*

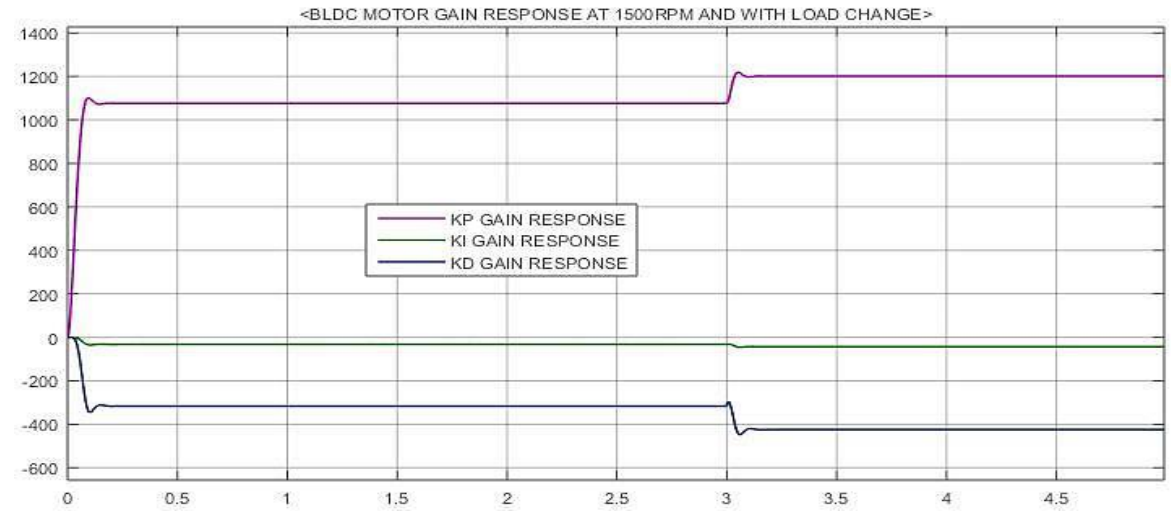

***Figure 34:**.Lyapunov stability method sudden load change Gain response at 1500rpm.*

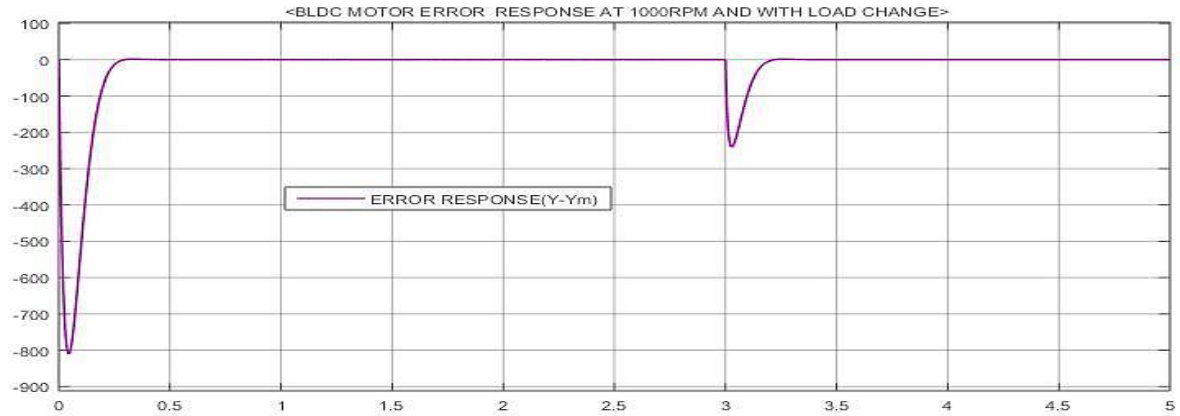

***Figure 35:**.Lyapunov stability method sudden load change, change in error response at 1000rpm.*

https://doi.org/10.46610/JOIIS.2021.v06i01.001

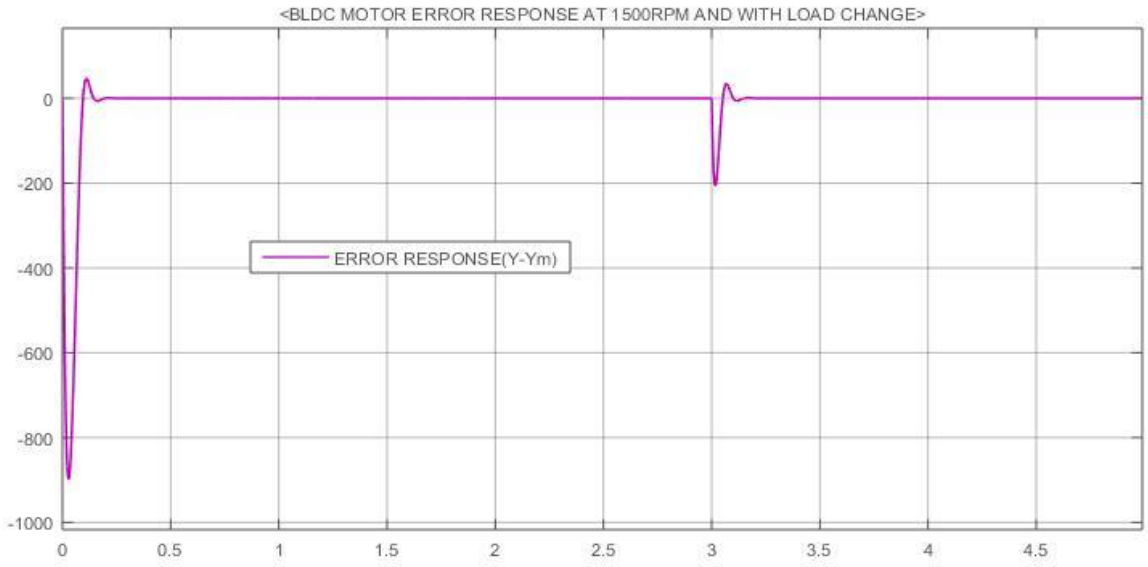

Figure 36: *Lyapunov stability method sudden load change, change in error response at 1500rpm.*

.

Lyapunov Stability Method Sudden Load Change Speed Tracking Response

Analyzing the addictiveness of the controllers is performed using a sine wave signal with a time period of 0.5 s and with constant amplitude. This can be interpreted as a repeated step response with each step lasting for a duration of 5 s and 50 Hz frequency duration. While it is common to use a single step function to examine ordinary of stability method to show how much tracks the speed response well is given in the given Fig. 37-39 below with Gain and change of error response given respectively.

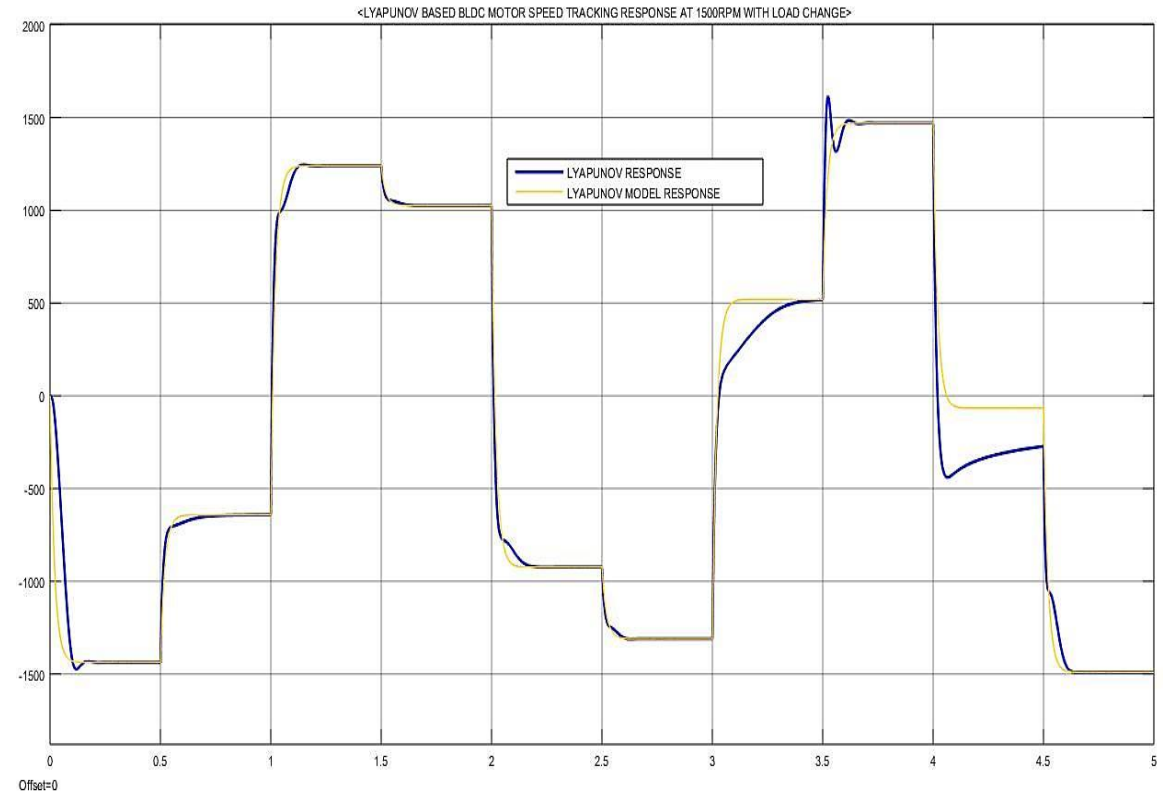

Figure 37: *Lyapunov stability method sudden load change, speed tracking response at 1500rpm.*

e-ISSN: 2456-9860
Volume-6, Issue-1 (January-April, 2021)
www.matjournals.com
https://doi.org/10.46610/JOIIS.2021.v06i01.001

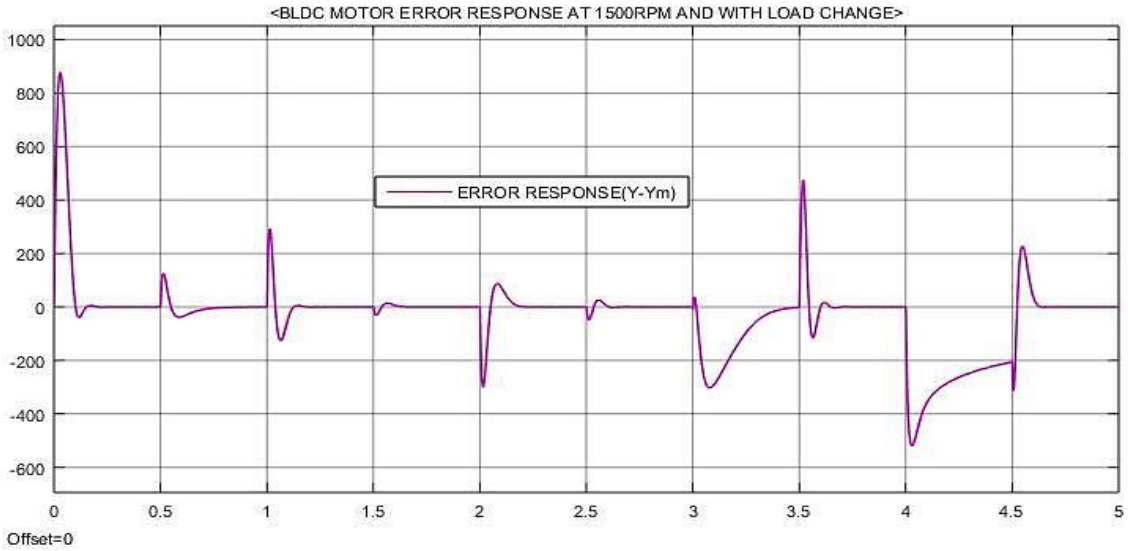

Figure 38: *Lyapunov stability method sudden load change, tracking change in error response at 1500rpm.*

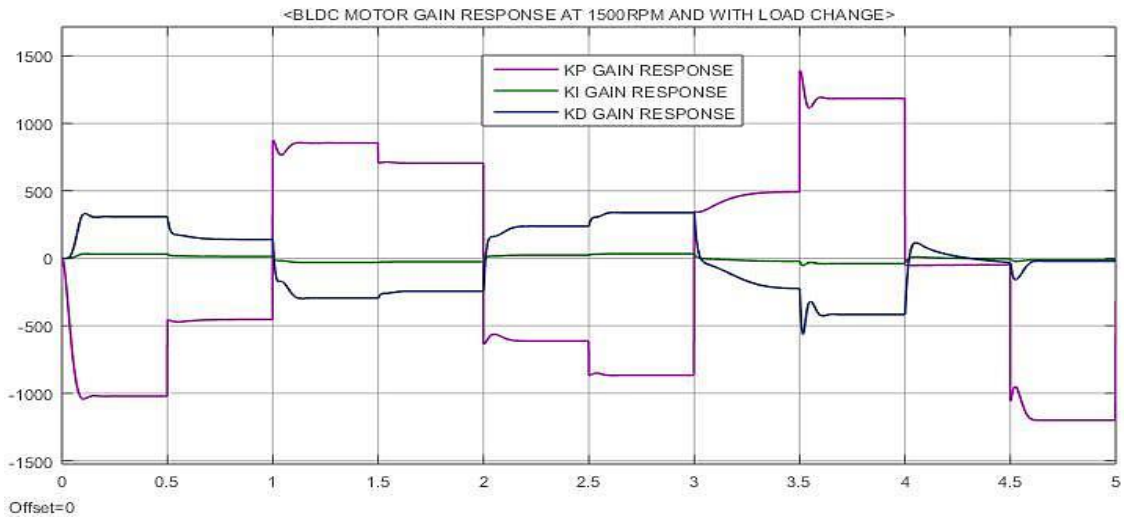

Figure 39: *Lyapunov stability method sudden load change Gain tracking response at 1500rpm.*

From the above Figures as we saw that the Lyapunov stability method shows a great speed tracking response and almost a zero change error between the plant and reference model which is a best requirement as a control system and a good Gain change is observed totally.

Response of Fuzzy Based Model Reference Adaptive Control

In order to investigate the effect of the proposed controller and to compare its performance with the conventional PID controller and simple MRAC controller, the Simulink model of the system employing these controllers was simulated and tasted and given in the Fig. 40 below with no load condition and with load condition is clearly established and an improved performance of the system is equipped with the proposed Fuzzy based MRAC controller with no load and with load of rated speed.

Fuzzy Based Model Reference Adaptive Control at No Load Condition

The overshoot of the system equipped with the proposed Fuzzy based MRAS controller is considered almost zero as compared to a percentage overshoot of simple MRAS and conventional PID controlled system during no-load condition.

https://doi.org/10.46610/JOIIS.2021.v06i01.001

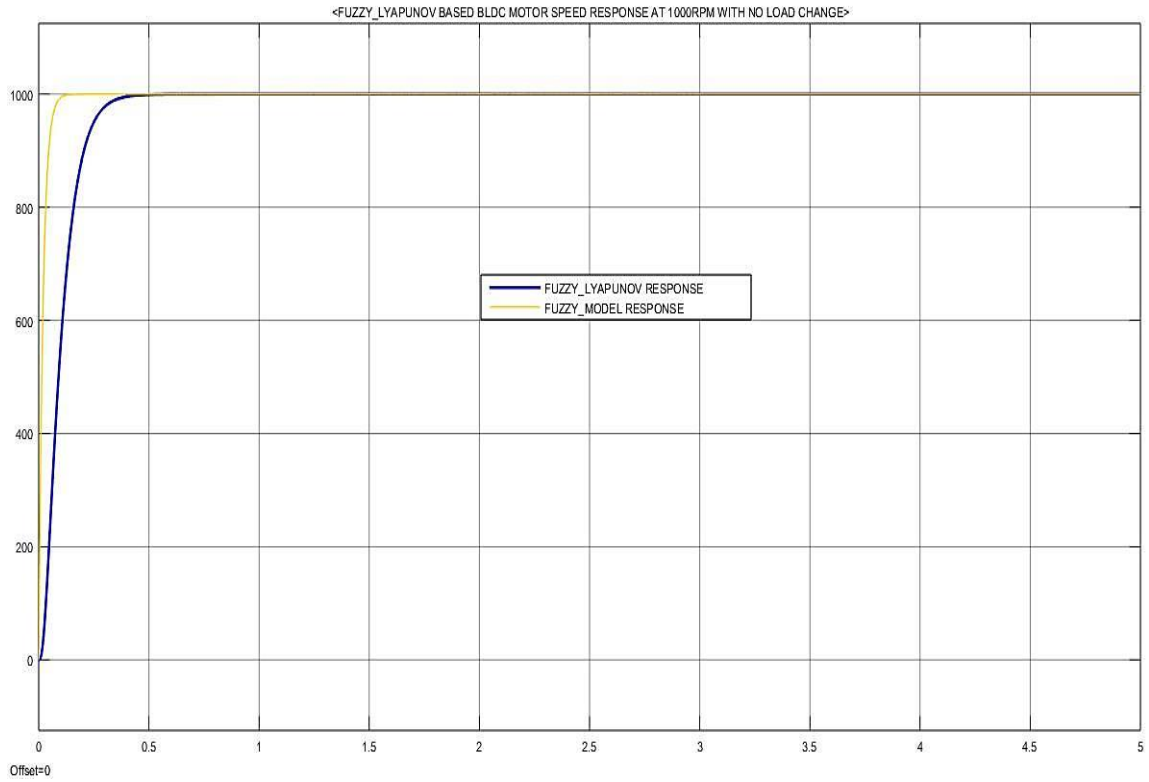

Figure 40: *Fuzzy based MRAS controller at no load speed of 1000rpm.*

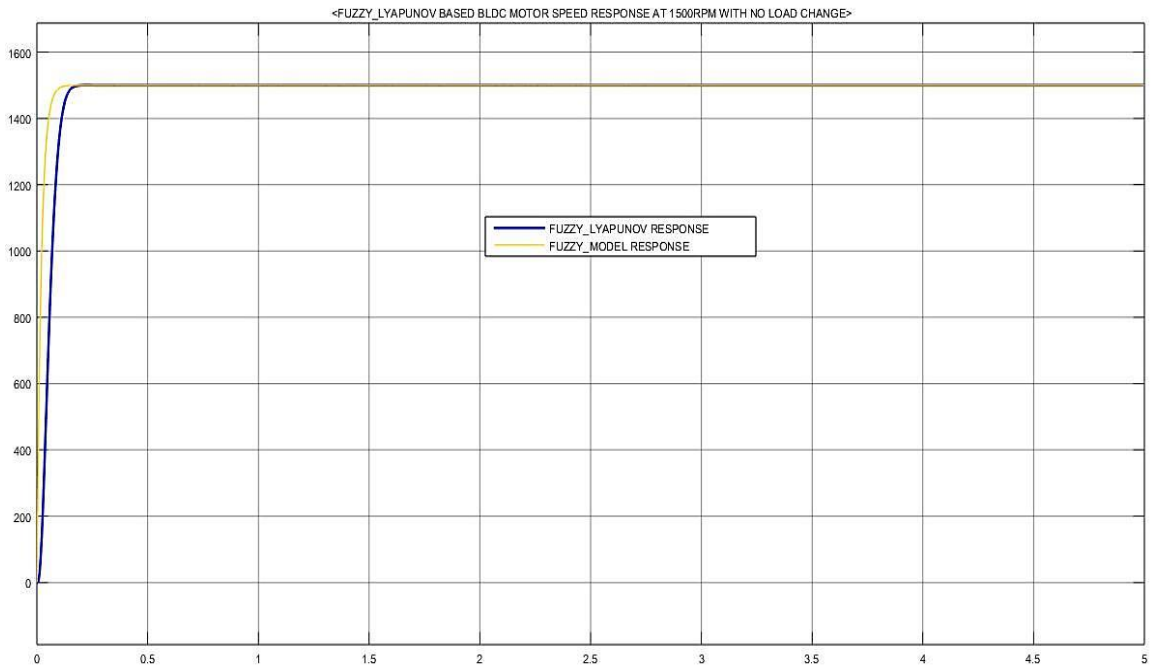

Figure 41: *Fuzzy based MRAS controller at no load speed of 1500rpm.*

From the above two Fig. 40-41 we have observed that the response of the close loop control system is stable and almost all adaptive with a comparative response of steady state response. While a Fuzzy control system is a learning system with lunges tic variable and witch is a human learning tool therefore the steady state response of the Fuzzy based MRAC system with no load applied on the plant, so Rise time is 0.169seconds, settling time is 0.491seconds and percentage over shoot is 0.501% at rated

https://doi.org/10.46610/JOIIS.2021.v06i01.001

speed of 1000rpm. And a Rise time is 0.0784seconds, settling time is 0.20seconds and a percentage overshoot of 0.505% at rated speed of 1500rpm is observed comparatively good robust response of the plant at no load respectively.

Fuzzy Based Model Reference Adaptive Control at Load Condition

The Fig. 42 and 43 below given indicates that how much the proposed system handles a load variation with the given rated speed of the plant when compared to with the others.

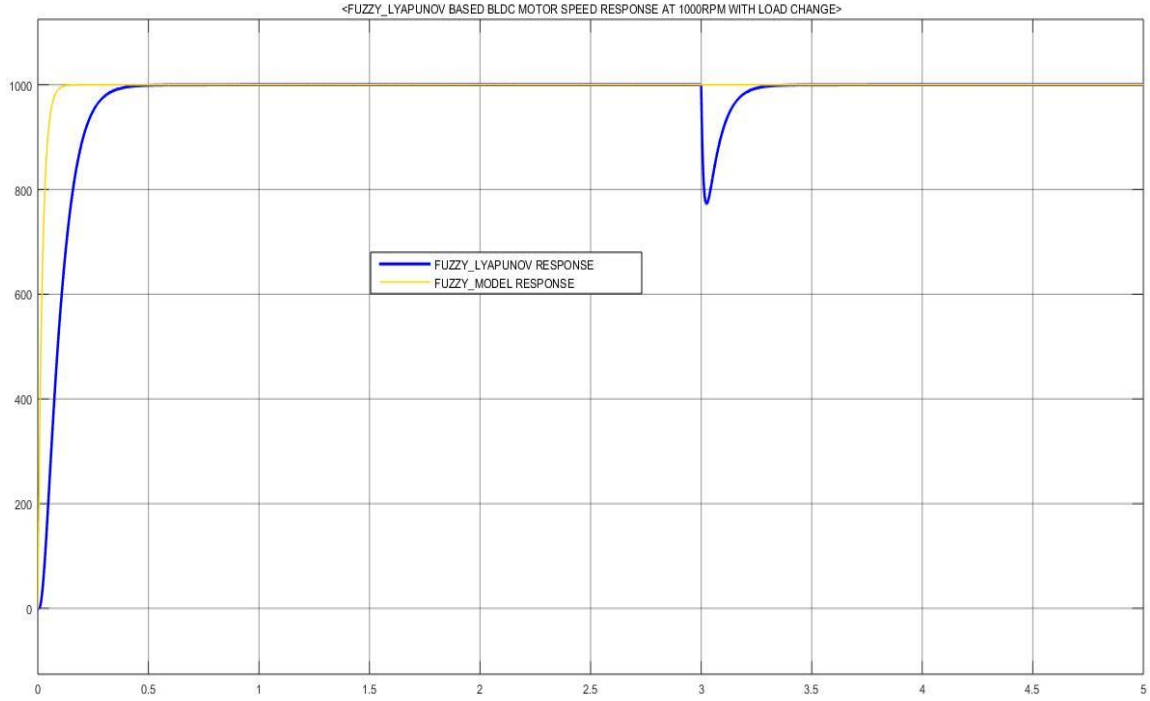

Figure 42: *Fuzzy based MRAS controller with load change and rated speed of 1000rpm.*

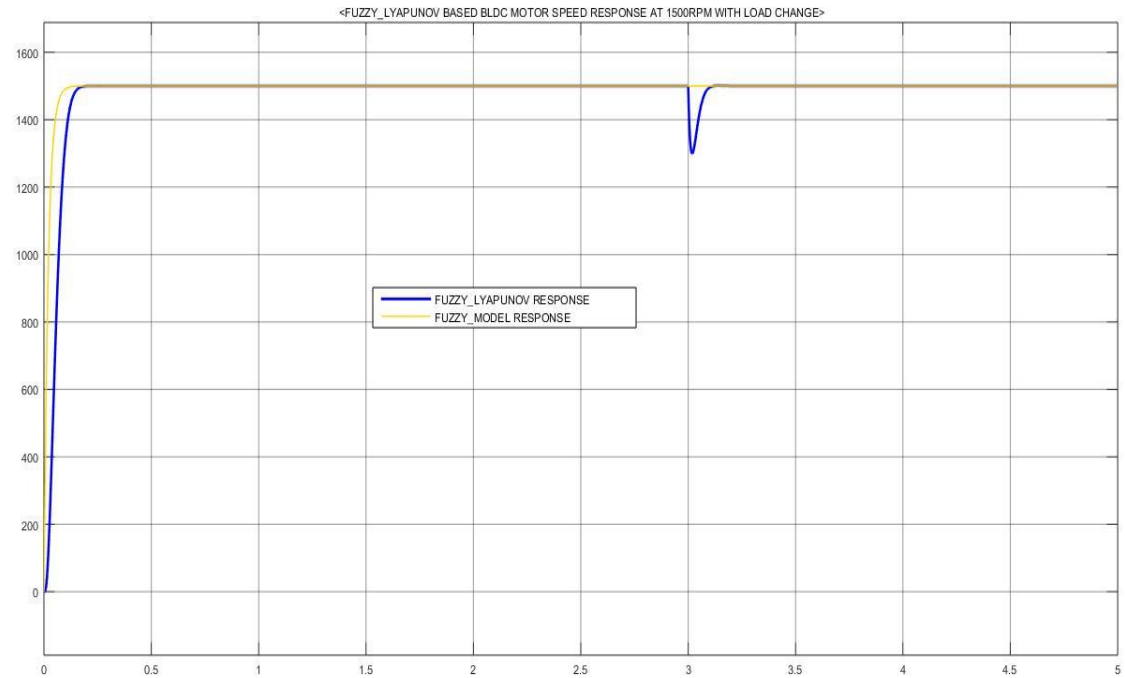

Figure 43: *Fuzzy based MRAS controller with load and rated speed of 1500rpm.*

https://doi.org/10.46610/JOIIS.2021.v06i01.001

Hence the above Fig. 42 and 43 show some considerable undershoot and a good speed response and good load rejection and stable response as adaptive control system and learning system.

Fuzzy Based Model Reference Adaptive Control at Unpredictable and Sudden Load Change

In order to further evaluate the response of the proposed controller configuration it has been evaluated under changing motor inertia and rated speed simultaneously at certain time. By increasing rated torque to 100Nm to show how much the system resists the unpredictable load disturbance or uncertain load disturbance and maintain the exact motor performance or operating condition. The following Fig. 44 and 45 shows the Simulink block diagram of system design with uncertain load disturbance and result performance at 1000rpm and 1500rpm rated speed and 100Nm of rated torque.

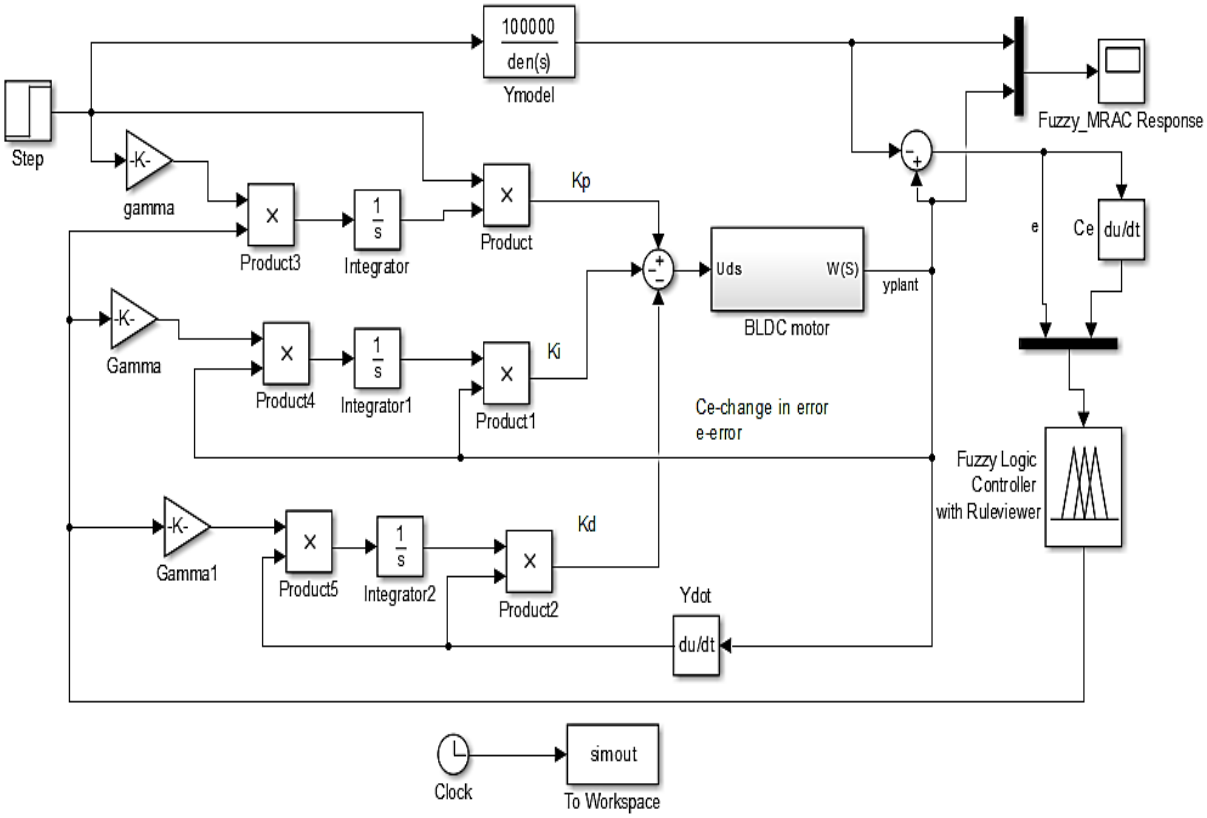

Figure 44: *Fuzzy based MRAC system with uncertain load change Tds.*

Sub block diagram of BLDC motor with uncertain load

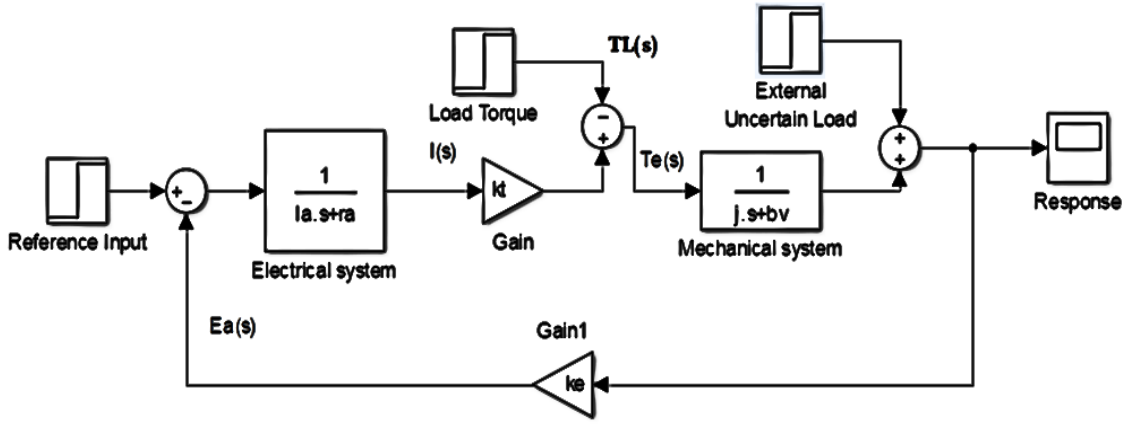

Figure 45: *Sub block diagram of BLDC motor with uncertain load change Td(s).*

e-ISSN: 2456-9860
Volume-6, Issue-1 (January-April, 2021)
www.matjournals.com
https://doi.org/10.46610/JOIIS.2021.v06i01.001

MATLAB Simulink Result of Uncertain Load Change at Rated Speed and 100Nm Rated Torque

Fig. 46 and 47 depicts the output of the controller for uncertain load change in rated torque and it can be observed from the figures of controller output varies rapidly with the change in inertia. The rise time is sudden increase with small change and can help in enhancing the speed of response of the controller to maintain the constant speed of the rated speed.

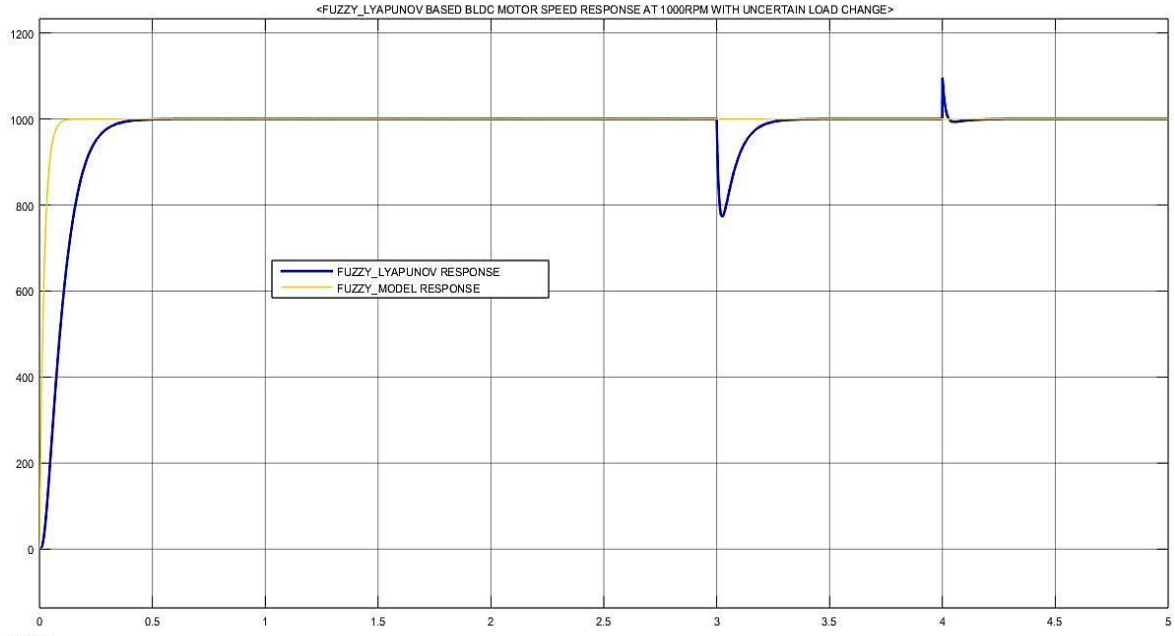

Figure 46: *Speed response of Fuzzy based MRAS controller at External sudden load and rated speed 1000rpm.*

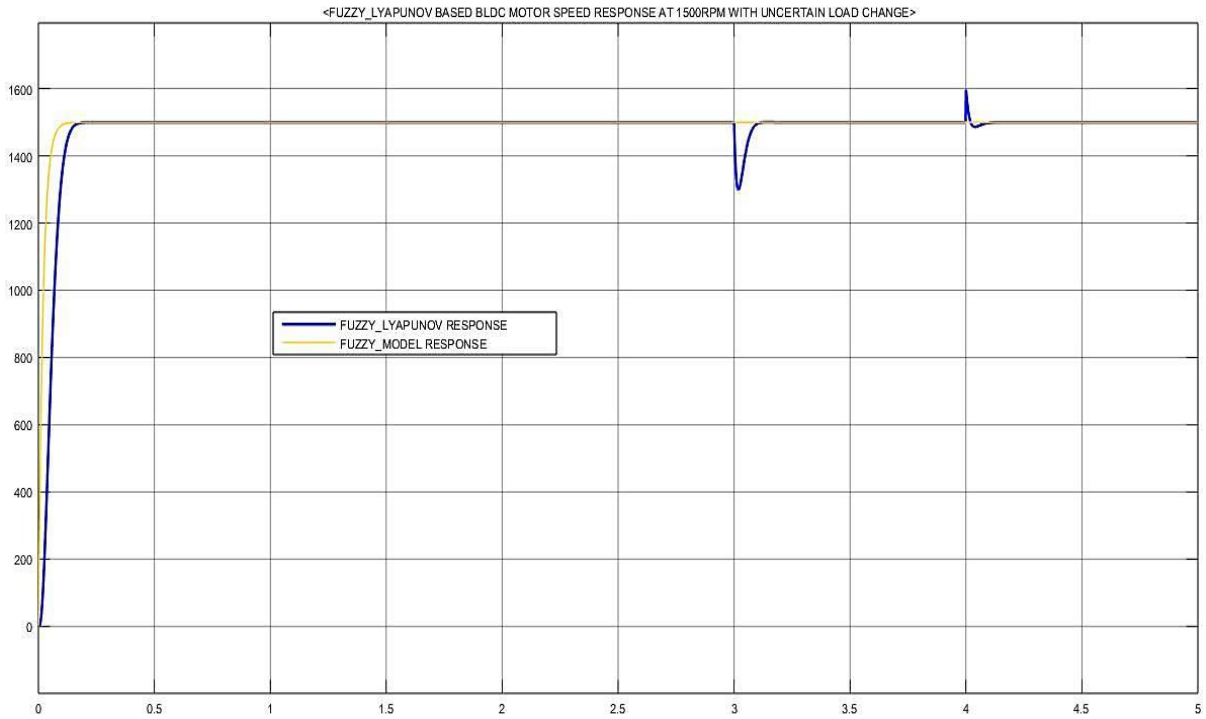

Figure 47:*.Speed response of Fuzzy based MRAS controller at External sudden load and rated speed 1500rpm.*

https://doi.org/10.46610/JOIIS.2021.v06i01.001

As shown in the above the performance of the fuzzy based MRAC controller with load condition of speed and Torque. The uncertain and sudden load torque applied on the system is 100-300 Nm and applied at 3 and 4 seconds to the close loop control system and it shows high stable response and fast load rejection due to that the offset overshoot also reduced instantly.

Proposed System Result Tracking and Result Compression

The given the following result shows how much the proposed control system sustain a load variation and track the reference model with a given speed and frequency oscillation to show the stability of the system with tracking speed and almost a zero error as a close loop control system. Therefore the following figures show the tracking speed response and some controller result compression of the system.

No Load Tracking Response of Proposed Controller

The following Fig. 48, 49 and 50 show how much the proposed system sustain load variation and give a stable response with compared to the others at steady state response of the plant at rated speed 1500rpm.

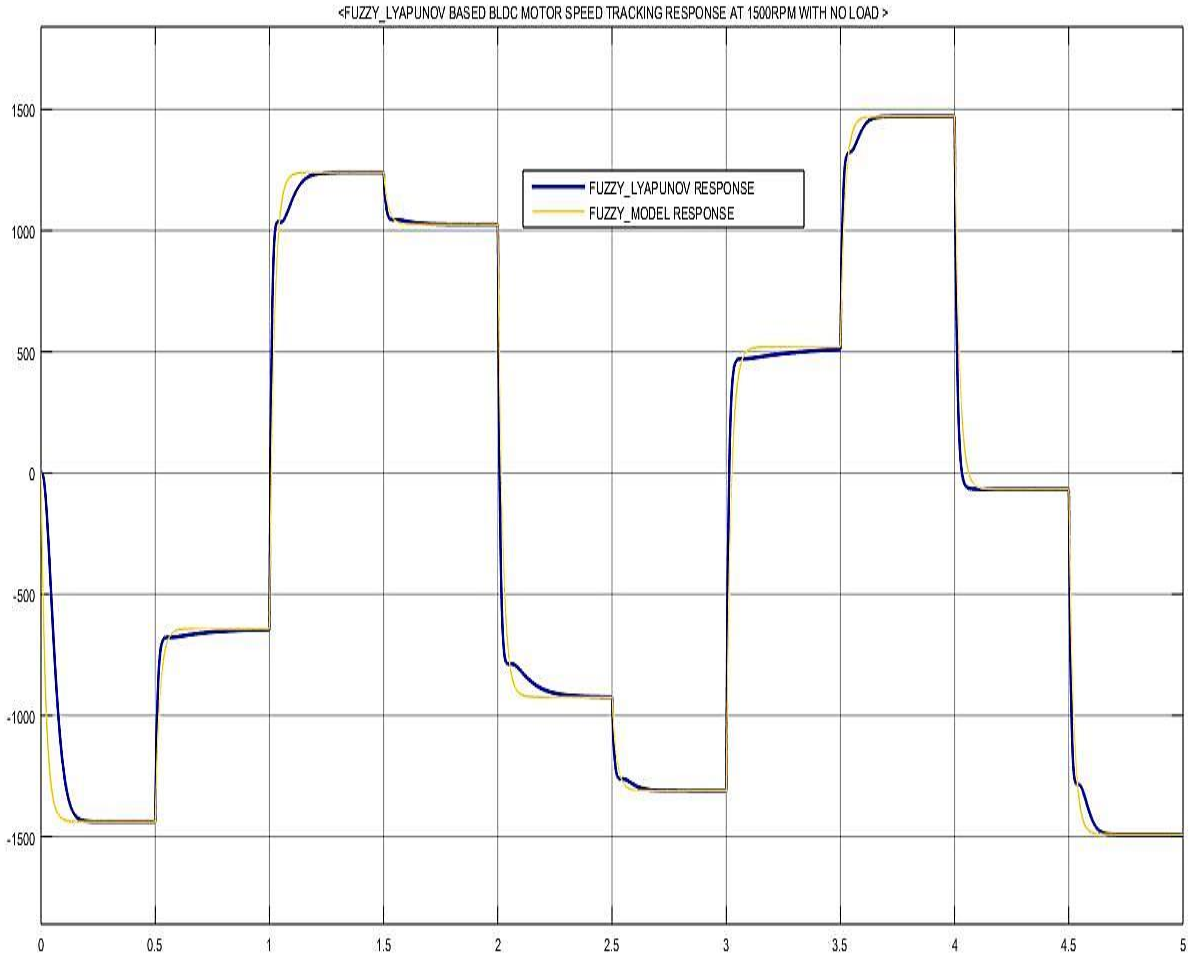

***Figure 48:**.No load speed tracking response of Fuzzy based MRAC system with rated speed of 1500rpm.*

https://doi.org/10.46610/JOIIS.2021.v06i01.001

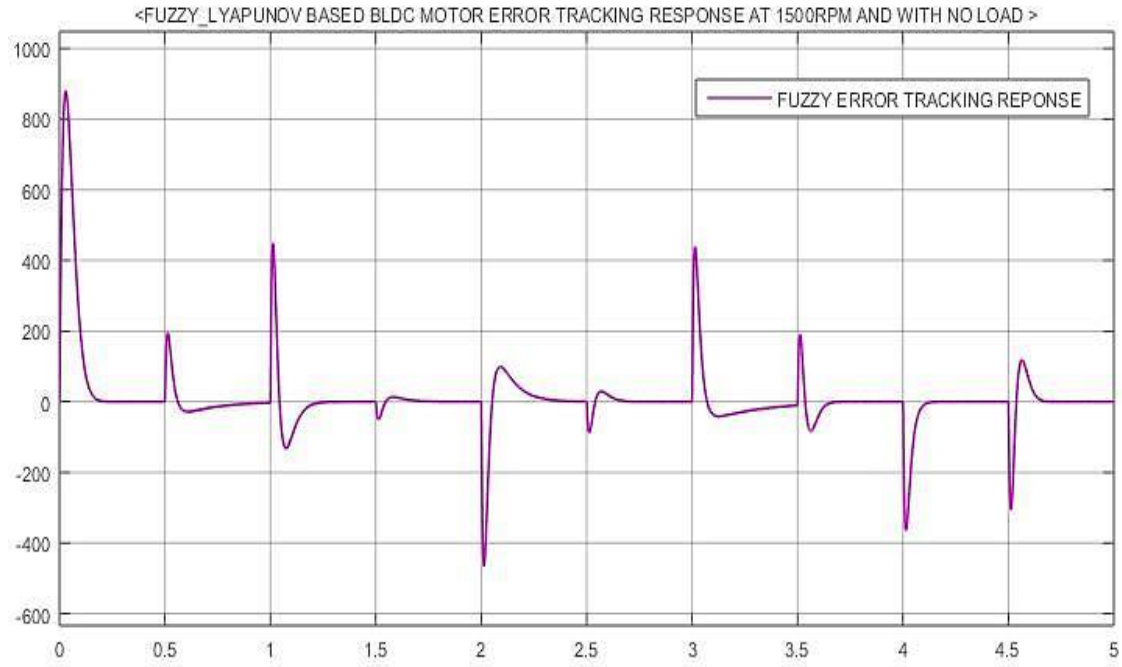

Figure 49: *No load error tracking response of Fuzzy based MRAC system at 1500rpm rated speed.*

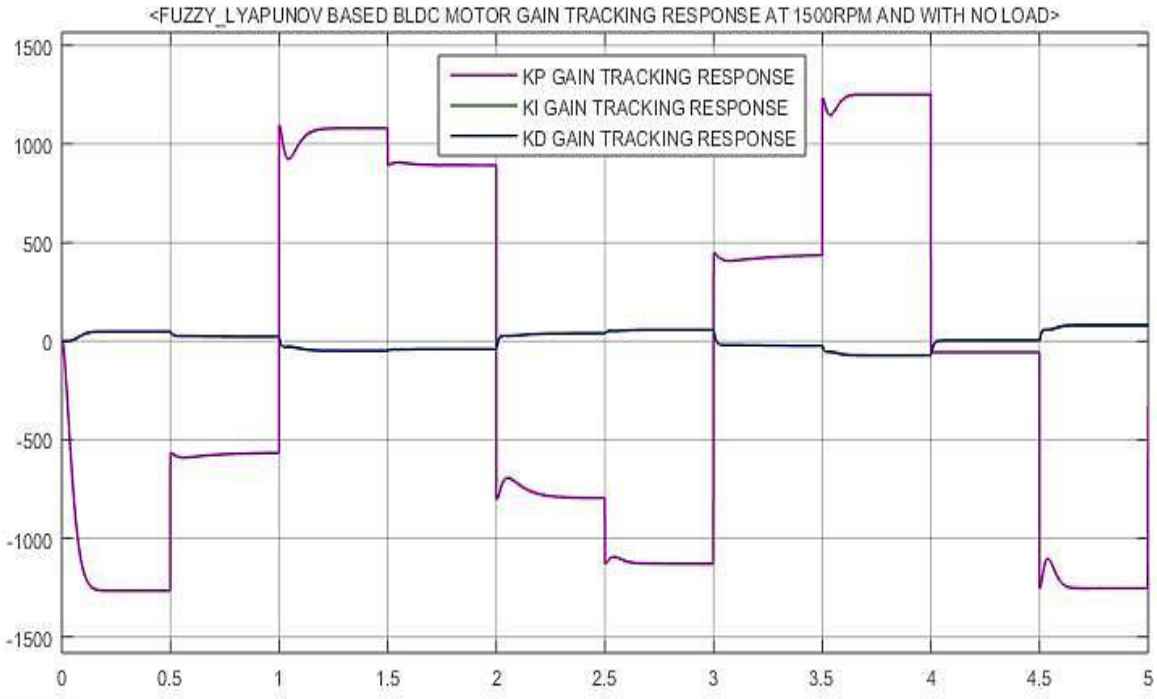

Figure 50:*.No load Gain tracking response of Fuzzy based MRAC system at 1500rpm rated speed.*

Load Tracking Response at 1500rpm and with Load Change of Proposed System

The following Fig. 51, 52 and 53 shows tracking response based on load change on the plant and the tracking response of proposed control system with a good response of tracking and almost a small error change observed as the result of the control system with load torque of 300Nm.

e-ISSN: 2456-9860
Volume-6, Issue-1 (January-April, 2021)
www.matjournals.com
https://doi.org/10.46610/JOIIS.2021.v06i01.001

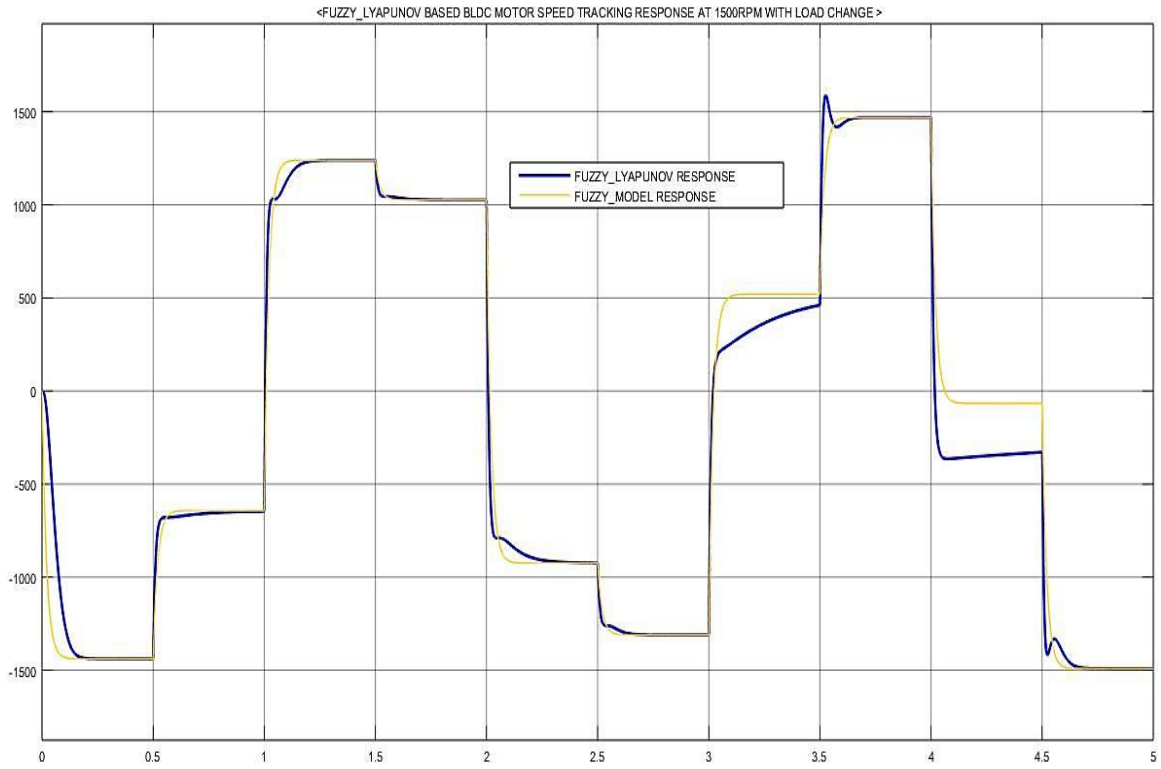

Figure 51: *Sudden load speed tracking response of Fuzzy based MRAC system.*

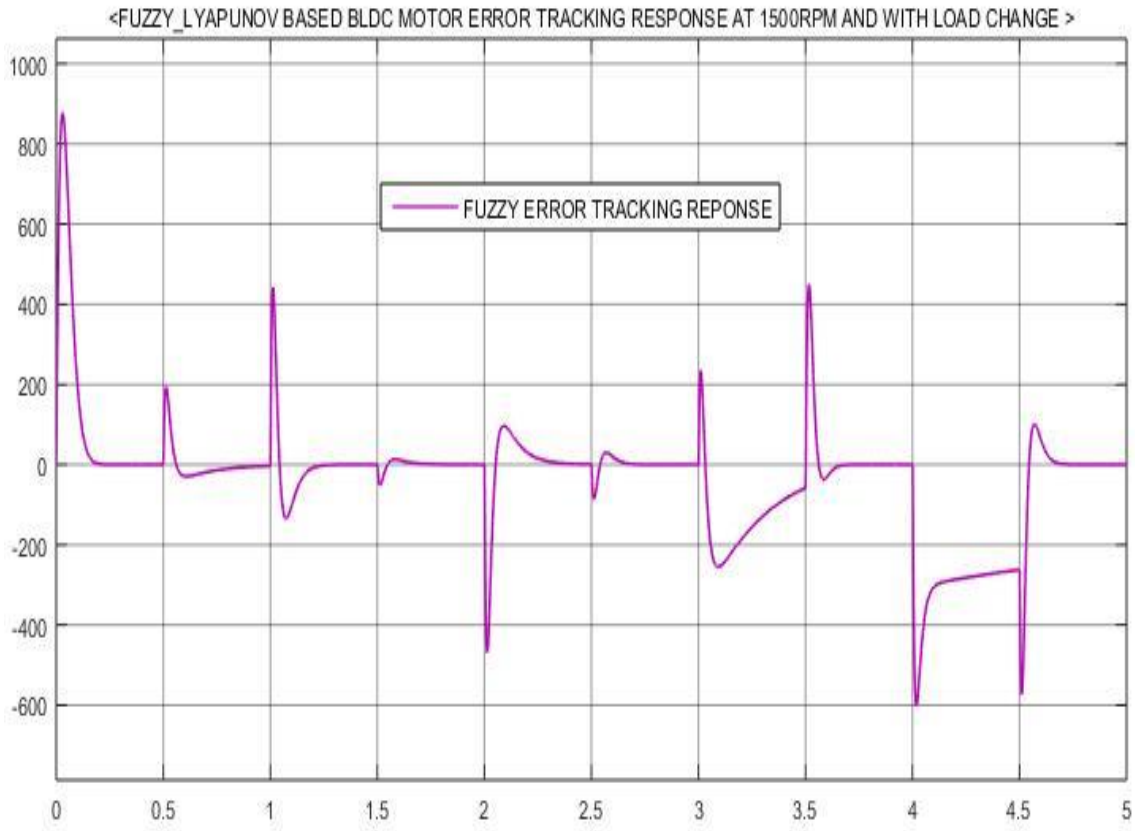

Figure 52: *Error tracking response of Fuzzy based MRAC system with load change at rated speed.*

https://doi.org/10.46610/JOIIS.2021.v06i01.001

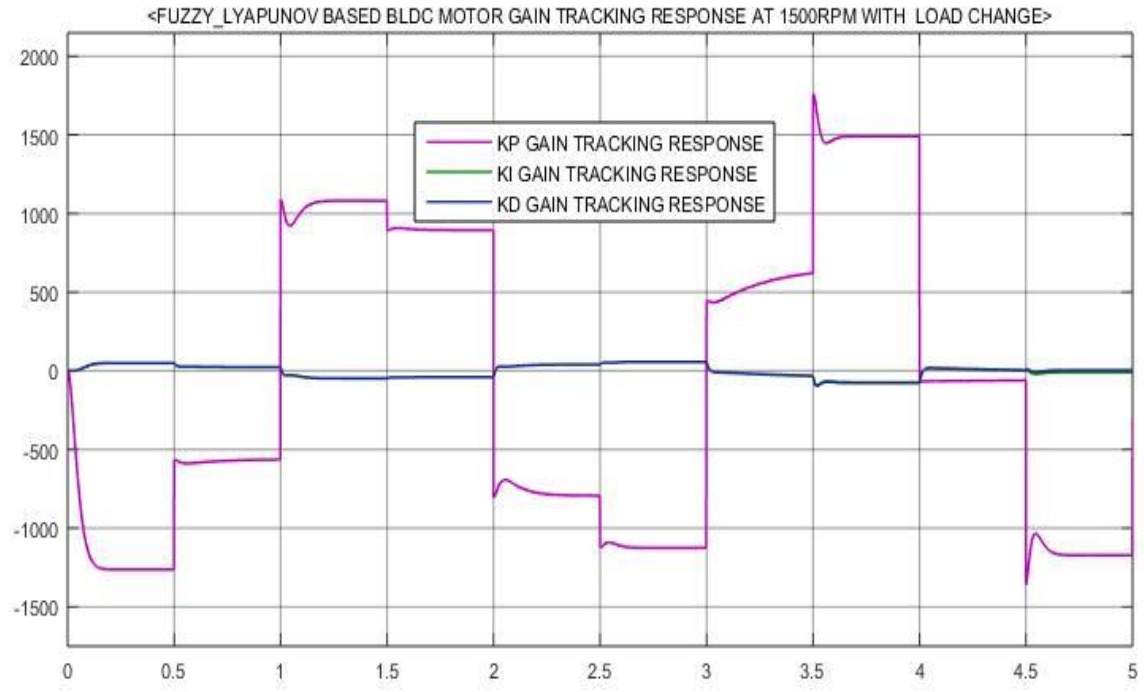

Figure 53: *Gain tracking response of Fuzzy based MRAC controller system with load change at rated speed.*

PROPOSED SYSTEM RESULT COMPARISONS

No Load Result Comparison at Rated Speed of 1500rpm

The following system result in Fig. 54 and 55 indicates the comparison of output signal of the plant which have been indicate in the above but to show how much the proposed system responds to the applied rated speed with no load condition in the same plane with steady state performance characteristics.

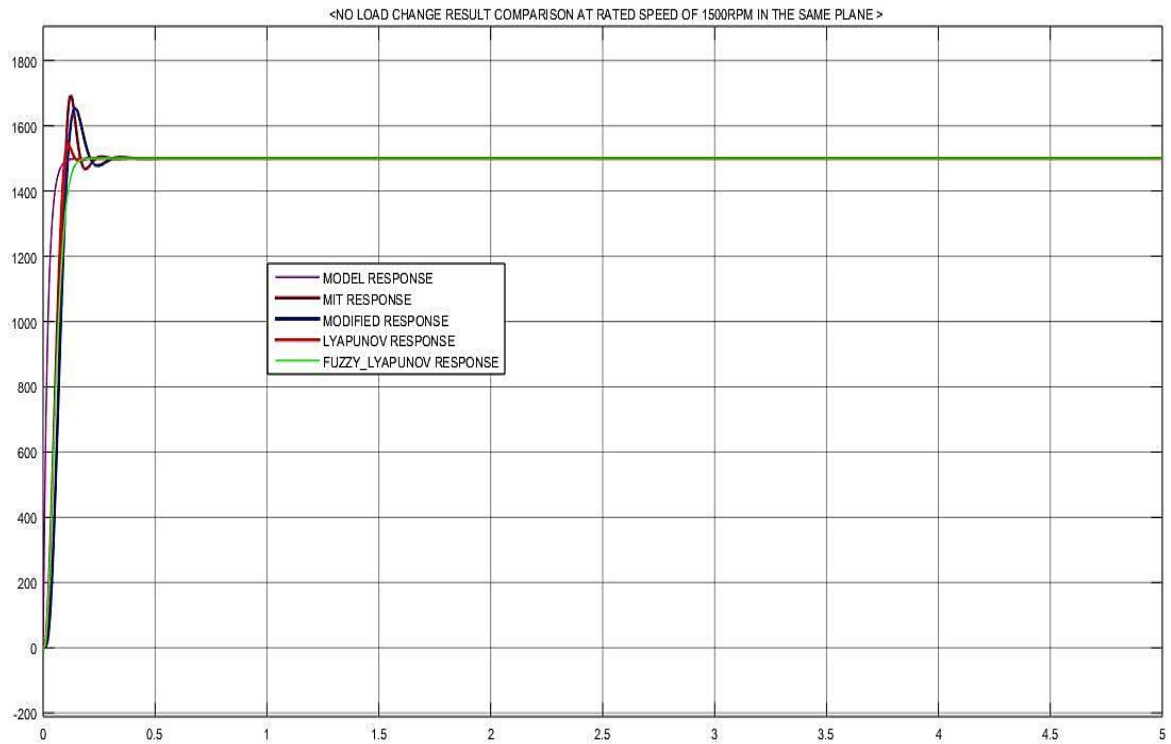

Figure 54: *No load performance result comparison of each control system.*

https://doi.org/10.46610/JOIIS.2021.v06i01.001

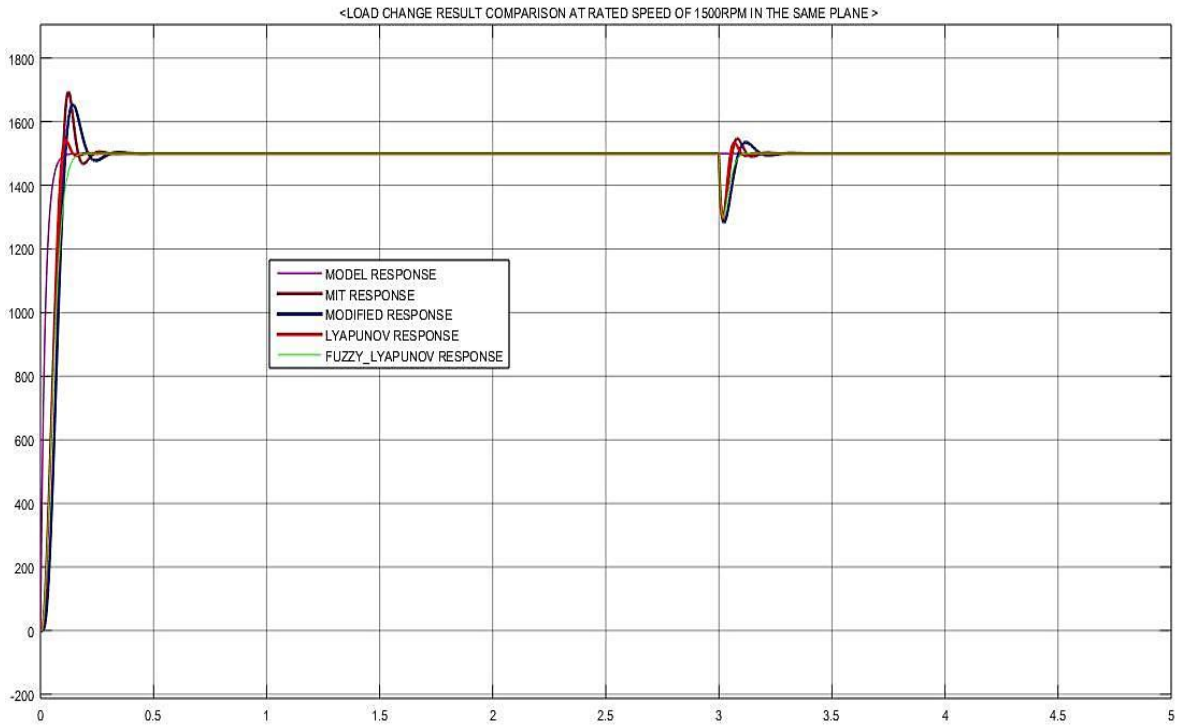

Figure 55: *Performance result comparison of each control system in the same plane with load change.*

Numerical Performance Comparison

The model reference adaptive control using Lyapunov stability method shows considerably reduced percentage overshoot and good tracking control with stability is ensured. Thus, Fuzzy based Model Reference Adaptive Control using Lyapunov Stability Method shows the best control and tracking performance as compared to PID controller and simple MIT rule methods so the given Table 3 below shows the comparison between the performance characteristics of each controllers at rated speed of the motor.

No Load Numerical Comparisons at Rated Speed

Table 3 No load numerical Comparison between the characteristics of each controller at 1500rpm rated speed.

Table 3: *No load comparison at 1500rpm.*

Performance Characteristics	PID controller	MRAS with MIT rule	MRAS With Lyapunov Stability Method	Fuzzy based MRAS controller
Maximum Overshoot (%)	18.452	13.068	2.577	0.505
Rise time (sec)	0.00552	0.0567	0.0596	0.0784
Settling time (sec)	0.012	0.4580	0.195	0.200
Preshoot (%)	0.595	0.568	0.515	0.505
Undershoot (%)	-3.436	2.090	1.513	1.433

e-ISSN: 2456-9860
Volume-6, Issue-1 (January-April, 2021)
https://doi.org/10.46610/JOIIS.2021.v06i01.001

Load Change Based Numerical Comparisons at 1500rpm Rated Speed

Table 4 load change based performance comparisons at rated speed and Load change at rated torque and also external uncertain load.

Table 4: *Load change based performance comparisons at rated speed.*

Performance Characteristics	PID controller	MRAS with MIT rule	MRAS With Lyapunov Stability Method	Fuzzy based MRAS controller
Maximum Overshoot (%)	18.452	13.068	2.577	0.474
Rise time (sec)	0.00255	0.0565	0.0596	0.0784
Settling time (sec)	0.01214	3.41	3.30	3.102
Preshoot (%)	0.595	0.568	0.515	0.505
Undershoot (%)	-3.295	2.064	1.656	1.502

From numerical performance comparison characteristics, a Fuzzy based MRAS controller shows better performance result and as given in the above figures and tables result of performance listed than simple MRAS and conventional PID controller, only some percentage undershoot is observed.

CONCLUSION

The show of BLDC engine is created with its energetic characteristics and a controller is planned by utilizing PID controller, Demonstrate Reference Versatile controller calculation with MIT run the show as well as Lyapunov Solidness strategy and Soft based MRAC with Lyapunov consistent quality methodology such that the speed control is gotten and is executed utilizing MATLAB/Simulink program. A relative think about between these three strategies were experienced and which appears that the Fluffy based Demonstrate Reference Versatile controller with the Lyapunov Solidness strategy appears way better comes about because it reduces the greatest overshoot conjointly disturbances are diminished nearly rejected. At that point there's significant decrease in relentless state blunder as well as settling time with a few undershoot thought. The stability of the system is also ensured using this type of controller and we have improved the existing system based on the numerical analysis and accurate percentage overshoot with god steady state response.

ACKNOWLEDGEMENT

This work was financially supported by Jimma Institute of technology, Jimma University Ethiopia for the research scholars.

CONFLICTS OF INTEREST

The authors declare that there is no conflict of interest regarding the publication of this paper

REFERENCES

1. Vinod Kr Singh Patel, A.K.Pandey (2005). Modelling and Simulation of Brushless DC Motor Using PWM Control Technique. *International Journal of Engineering Research and Applications*, 3 (3), 612-620, Available at: http://citeseerx.ist.psu.edu/viewdoc/download?doi=10.1.1.419.2698&rep=rep1&type=pdf.

2. K. Ang, G. Chong, Y. Li, (2005). PID control system analysis, design, and technology. *IEEE Transaction on Control System Technology*, 13 (4), 559-576, Available at: 10.1109/TCST.2005.847331.
3. Atef Saleh Othman Al-Mashakbeh (2009). Proportional Integral and Derivative Control of Brushless DC Motor. *European Journal of Scientific Research*, ISSN 1450-216X, 35 (2), 198-203, Available at: https://nanopdf.com/download/pid-bldc-control_pdf.
4. Manafeddin Namazov (2010). DC motor position control using fuzzy proportional-derivative controllers with different defuzzification methods. *Turkish Journal of Fuzzy Systems*, 1 (1), 36-54, eISSN: 1309–1190, Available at: http://dspace.bhos.edu.az/jspui/bitstream/123456789/996/1/DC%20motor%20position%20control.pdf.
5. Uzair Ansari; Saqib Alam, Syed Minhaj un Nabi Jafri (2011). Modelling and Control of Three Phase BLDC Motor using PID with Genetic Algorithm. *UK Sim 13th International Conference* on Modelling and Simulation, (pp189-194), Cambridge, UK, Available at: https://doi.org/10.1109/UKSIM.2011.44.
6. Anjali.A.R (2013). Control of Three Phase BLDC Motor Using Fuzzy Logic Controller. *International Journal of Engineering Research &Technology* (IJERT), 2 (7), ISSN: 2278-0181. Available at: https://www.ijert.org/research/control-of-three-phase-bldc-motor-using-fuzzy-logic-controller-IJERTV2IS70269.pdf.
7. R. Kandiban, R. Arulmozhiyal (2012). Design of Adaptive Fuzzy PID Controller for Speed control of BLDC Motor. *International Journal of Soft Computing and Engineering (IJSCE)*, 2 (1), 386-391, ISSN: 2231-2307, Available at: http://citeseerx.ist.psu.edu/viewdoc/download?doi=10.1.1.648.6978&rep=rep1&type=pdf.
8. J. J. E.Slotine, W. Li (1989).Composite Adaptive Control of Robot manipulators. Automatica, *Elsevier*, 25 (4), 509-519, Available at: https://doi.org/10.1016/0005-1098(89)90094-0.
9. Adel A.El-samahy & Mohamed A.Shamseldin, (2018). BLDC motor tracking control using self-tuning fuzzy PID control and model reference adaptive control. Ain Shams University, *Ain Shams Engineering Journal*, 9 (3), 341-352, Available at: https://doi.org/10.1016/j.asej.2016.02.004.
10. Thasneem M.S, Shalu George K. (2017).Speed Control of Brushless DC Motor Using Model Reference Adaptive Control. *International Journal of Advanced Research in Electrical, Electronics and Instrumentation Engineering*, 6 (5), Available at: https://www.ijareeie.com/upload/2017/may/12_IJAREEIE_Paper%20_17_.pdf.
11. Lei Jin-li (2014). Adaptive Control for Brushless DC Motor Based on Fuzzy Inference. *Telkomnika Indonesian Journal of Electrical Engineering*, 12 (5), 3392 - 3398, Available at: https://www.researchgate.net/publication/274476920_Adaptive_Control_for_Brushless_DC_Motor_Based_on_Fuzzy_Inference.
12. M. A. Shamseldin, A. M. A. Ghany, M. & A. A. Ghany (2018). Performance Study of Enhanced Non-Linear PID Control Applied on Brushless DC Motor. *International Journal of Power Electronics and Drive System* (IJPEDS), 9 (2), 536–545, Available at: http://repository.fue.edu.eg/xmlui/handle/123456789/5084.
13. Murali Dasari, A Sreenivasula Reddy, M Vijayakumar, (2017). Modeling of a commercial BLDC motor and control using GA-ANFIS tuned PID controller. *IEEE International Conference on Innovative Research in Electrical Sciences* (IICIRES), Nagapattinam, India, Available at: https://doi.org/10.1109/IICIRES.2017.8078305.
14. Adel A.El-samahy., Mohammed A.Shamseldin, (2018). Brushless DC Motor tracking control using self-tuning fuzzy PID control and model reference adaptive control. *Ain Shams Engineering Journal*, 9 (3), 341-352, Available at: https://doi.org/10.1016/j.asej.2016.02.004.
15. Chang-liang Xia (2012). Permanent Magnet Brushless DC Motor Drives and Controls. *John Wiley & Sons Singapore*, First Edition, pp26-52, Science Press.

e-ISSN: 2456-9860
Volume-6, Issue-1 (January-April, 2021)

https://doi.org/10.46610/JOIIS.2021.v06i01.001

Published 2012, Available at: https://download.e-bookshelf.de/download/0000/6294/15/L-G-0000629415-0002365029.pdf.

16. Stephen L. Herman (2014). Industrial Motor Control. *Thomson/Delmar Learning*, Australia, ISBN-13: 978-1133691808, ISBN-10: 1133691803. Available at: https://books.google.co.in/books?hl=en&lr=&id=ndkWAAAAQBAJ&oi=fnd&pg=PP1&dq=16.%09Stephen+L.+Herman+(2014).
17. Paul C Krause (1986). Analysis of Electric Machinery. *McGraw-Hill series in electrical engineering*, Power and Energy, The University of Michigan, ISBN-10: 0070354367, ISBN-13:9780070354364. Available at: http://php7.bluebus.com.eg/cgi-bin/file.php?article=analysis.of.electric.machinery.krause.manual.solution&code=79ee2fb21f6135fd1f48ec76939a7818.
18. Pillay, P., Krishnan, R. (1989). Modeling, simulation, and analysis of permanent-magnet motor drives, part I: the permanent-magnet synchronous motor drive. *IEEE Transactions on Industry Application*, 25 (2), 274-279, Available at: https://doi.org/10.1109/28.25542.
19. Jingde Gao., Linzheng Zhang., Xiangheng Wang. (2009). AC Machine Systems: Mathematical Model and Parameters, Analysis, and System Performance. *Tsinghua University Press*, Beijing (China), ISBN: 978-7-302-19342-5, Springer Dordrecht Heidelberg London New York, ISBN: 978-3-642-01152-8, e-ISBN: 978-3-642-01153-5., Available at: https://www.springer.com/gp/book/9783642011535#aboutBook.
20. Paul Krause, Oleg Wasynczuk ,Scott Sudhoff , Steven Pekarek.(2013). Analysis of Electric Machinery and Drive Systems, Third Edition, *Wiley-IEEE Press (Wiley online Library)*, ISBN: 9781118524336, Available at: https://doi.org/10.1002/9781118524336.fmatter.
21. Mohamed. A.Shamseldin, M. Abdullah Eissa, & Adel. A. EL-Samahy, (2015). A Modified Model Reference Adaptive Controller for Brushless DC Motor. *17th International Middle East Power Systems Conference*, Mansoura University, Egypt, December, (pp15-17), Available at: https://www.researchgate.net/publication/288503637_A_Modified_Model_Reference_Adaptive_Controller_for_Brushless_DC_Motor.
22. C. Mohankrishna, N. Rajesh Kumar Gowd, A. Ramesh, & G. Subba Rao Gupta (2016). Modelling and Simulation of BLDC Motor Using State Space Approach. *International Journal of Innovative Research in Electrical, Electronics, Instrumentation and Control Engineering*, 4 (5), ISSN: 2321-2004, Available at: https://www.scribd.com/document/369781006/IJIREEICE-123-pdf.
23. Murali Dasari et al,(2019). GA-ANFIS PID compensated model reference adaptive control for BLDC motor. *International Journal of Power Electronics and Drive System* (IJPEDS),10 (11), 265-276, Available at: https://search.proquest.com/openview/c66bc318a922581a78df9d026af82b53/1?pq-origsite=gscholar&cbl=1686343.
24. Brijesh Singh et al, (2010). Intelligent PI Controller for Speed Control of D.C. Motor. *International Journal of Electronic Engineering Research*, ISSN 0975 – 6450, 2 (1), 87–100. Available at: https://www.researchgate.net/profile/Surya-Prakash-7/publication/238726011_Intelligent_PI_Controller_for_Speed_Control_of_DC_Motor/links/5693e35c08aeab58a9a2bbbe/Intelligent-PI-Controller-for-Speed-Control-of-DC-Motor.pdf.

NOMENCLATURE

Specifications of BLDC motor used for simulation is given in table below.

PARAMETERS	VALUES
Rated Power	6000W
Rated Voltage	315V
Rated Current	20A

e-ISSN: 2456-9860
Volume-6, Issue-1 (January-April, 2021)

www.matjournals.com
https://doi.org/10.46610/JOIIS.2021.v06i01.001

Rated speed	1000-1500 rpm
Rated Torque	100N-m
Stator Resistance	0.43Ω
Stator Inductance	0.00255H
Inertial Constant	0.0011
Viscous Friction Coefficient	0.005